



Paper 6.1

Thermal Gradient Effects on Ultrasonic Flowmeters in the Laminar Flow Regime

**Gregor Brown
Cameron**

**Don Augenstein
Cameron**

**Herb Estrada
Cameron**

**Chris Laird
Cameron**

**Terry Cousins
Cameron**



Thermal Gradient Effects on Ultrasonic Flowmeters in the Laminar Flow Regime

**Gregor Brown, Cameron
Don Augenstein, Cameron
Herb Estrada, Cameron
Chris Laird, Cameron
Terry Cousins, Cameron**

1 INTRODUCTION

With the rising oil price and depletion of conventional oil reserves the production of heavy oil is becoming increasingly common. The high viscosity of heavy oils presents measurement challenges for most types of flow meter.

Ultrasonic meters can be used for measurement of high viscosity oils. In order to do so there are two challenges that are commonly acknowledged: (1) the need to overcome increased signal attenuation; and (2) the requirement to operate accurately through the transition region where velocity profiles vary dramatically. It is often assumed that accurate measurement in the laminar regime is less difficult than in transitional flow. However, relatively little information on the performance of ultrasonic meters in laminar flow has been published.

This paper focuses on experimental test results obtained in laminar conditions where the oil temperature and ambient temperature are different. Tests have been performed in a variety of situations, with different installation conditions, meter types and with insulated meter runs. An explanation of the mechanism by which thermal gradients affect the performance of ultrasonic flow meters is provided, supported by diagnostic data. Results from tests on a novel flow conditioner, designed to improve performance of ultrasonic meters in the laminar regime, are also presented.

2 BACKGROUND

In the majority of industrial applications of ultrasonic flow meters, the flow is turbulent. Many text books and technical review papers that deal with ultrasonic meters barely mention laminar flow, and fail to speculate about performance issues in that regime. Numerical calculations of the 'hydraulic correction factor' or 'flow coefficient' for fully developed laminar flow show it as single valued, being 0.75 for a diameter path [1] and close to 1 for Gauss-Jacobi integration with four paths [2], suggesting that (in the absence of upstream bends etc), the calibration of an ultrasonic meter does not vary in laminar flow.

With increasing focus on heavy oils, a need has arisen to achieve custody transfer levels of uncertainty with products of high viscosity flowing at relatively low Reynolds numbers. In order to achieve the performance required there are two obstacles that are generally acknowledged: (1) the need to overcome increased signal attenuation; and (2) the requirement to operate accurately through the transition region where velocity profiles vary dramatically.

By optimising meter body design, transducers, electronics and signal processing, the issues of high attenuation and the effects of transitional velocity profiles can be managed. By combining the right elements, this means that meters can operate through the turbulent and transition regions with viscosities in excess of 1000 cSt [2]. This might tend to suggest that measurement to custody transfer levels of uncertainty can be easily achieved in laminar flow. However, laminar flow has complexities of its own.

First let us deal with the issues of flow velocity profile. It is known that laminar flow can potentially require a long length of straight pipe before it becomes fully developed. Data in Miller's Internal Flow Systems [3] shows laminar flow in a pipe (following a smooth inlet from a

tank) reaching fully developed conditions in approximately 3 diameters at a Reynolds number of 100 but more than 50 diameters at a Reynolds number of 2,000. So for Reynolds numbers below say 300, the upstream straight length requirements should not be particularly demanding. For Reynolds numbers approaching transition, profile distortion may persist for much longer. However, we know that velocity profile distortions can be dealt with by use of multiple paths. Furthermore, conventional flow conditioners and/or reducing nozzles can also be used to condition the profile. So it can be reasoned that flow profile distortions are not particularly problematic in laminar flows when an appropriate multipath meter design is used.

Now let us consider what other issues may arise in laminar flow. In Miller's book [3] the following statement is made:

"In internal flow, turbulence is a phenomenon which is considered desirable in some situations and undesirable in others; for instance, it is responsible for the majority of pressure losses but it also makes many heat transfer, mass transfer and combustion processes economically possible."

In the book Boundary Layer Theory [4], in the chapter on *Thermal boundary layers in laminar flow*, Schlichting gives the following example:

"If we imagine a solid body which is placed in a fluid stream and which is heated so that its temperature is maintained above that of the surroundings then it is clear that the temperature of the stream will increase only over a thin layer in the immediate neighbourhood of the body and over a narrow wake behind it."

It is clear therefore that the absence of turbulent mixing in laminar flows can result in thermal boundary layers where the temperature in a thin layer next to the pipe wall varies between the pipe wall temperature and the 'core' temperature.

This issue is of particular relevance when considering the production and transportation of heavy crude oils. Take for example transportation of Venezuelan Merey crude. Using the data from the EI database [5], the viscosity this crude oil at 20 °C is around 2,091 cSt, whereas at 40 deg °C it is around 418 cSt. For a flowrate of 2000 m³/hr in a 16-inch pipe, the resulting pressure loss is about 1.62 bar per 100 m of pipe at 20 °C, and only 0.32 bar per 100 m at 40 °C. This illustrates that for ease of transportation, it makes sense to maintain heavy crudes at temperatures above ambient.

The paper by Hogendoorn et al [6] presented at the 2009 North Sea Flow Measurement Workshop explored the issue of thermal boundary layers in laminar flow by means of computational fluid dynamics (CFD) simulations. Two-dimensional simulations were performed to reduce computational effort. The CFD simulations were used to evaluate the effects of the thermal gradients on the velocity profiles upstream of the meter and in the measurement section. These velocity profiles in the measurement section were in turn integrated according to a model of the ultrasonic meter, and the effects evaluated. It was concluded that the effects were generally small, with the extreme case of a 20 °C difference in temperature producing an error of less than 0.3 % in the meter reading. Hogendoorn's paper also included a test performed with a reasonably high viscosity oil, and a protruding gasket, the intention being that the gasket would simulate a velocity profile disturbance similar to that caused by thermal gradients. This test showed no significant impact on the meter calibration, confirming that the changes in velocity profile caused boundary layer disturbances (including thermal gradients) have little impact on some models of multipath ultrasonic meter.

However, as will be shown in this paper, changes in velocity profile are only part of the story, and as it turns out, not the most important part. Cameron's evaluation of thermal gradient effects began several years ago with a programme of laboratory testing at low Reynolds numbers, and was later supplemented this by CFD analysis. By adopting this approach it was discovered that velocity profile changes in laminar flow are of little concern, but that another physical mechanism can potentially result in significant errors due to the presence of thermal gradients.

3 PRELIMINARY INVESTATIONS INTO LAMINAR FLOW

Most available calibration facilities are not particularly suitable for testing industrial ultrasonic meters in laminar flow, particularly if a variation in fluid temperature is desirable. Take for example a 6-inch meter that we wish to calibrate over a 5:1 turndown in the laminar regime. At a nominal velocity of 5 m/s the oil would have to have a viscosity of close to 400 cSt to keep the Reynolds number below 2,000. If we wanted to achieve the same at temperature of 40 °C, the oil would have to have a viscosity of around 1,900 cSt at 20 °C. This general requirement combining availability of viscous product plus control of fluid temperature is rare.

In early 2005, NEL purchased a quantity of Primol 352 for use in their oil flow calibration facilities. This fluid initially had a viscosity of around 215 cSt at 20 °C, allowing laminar flow to be achieved at velocities below roughly 2.8 m/s at 20 °C and below 0.9 m/s at 40 °C. Although not ideal for laminar flow alone (as higher velocities are desirable), this fluid provided a good opportunity for testing through the laminar, transitional and turbulent regimes, complete with variation in temperature. Later a second product, Paraflex, was added to the range of stock oils at NEL, this oil having a viscosity of approximately 330 cSt at 20 °C, thus extending the range of tests conditions that can be obtained.

The facilities at NEL use a weighbridge as a primary standard, with PD meters used as secondary standards for the high viscosity oils. The use of two 8-inch PD meters in parallel allows maximum flowrate in the region of 500 m³/hr when using the most viscous product, dependent of course on the test line configuration.

The majority of tests described in this paper were conducted at NEL. As the test facilities are indoor, the ambient temperature was generally in the range of 18 to 22 °C.

Figure 1 below shows the results of a calibration performed at 20 °C at NEL using the Primol product. The meter used was a standard 6-inch Caldon LEFM 240C (full bore design) with four paths. It was installed with approximately 50 diameters of straight pipe upstream and no flow conditioning. The range of velocity covered by these test results is from 0.5 to 5 m/s.

The results in Figure 1 are presented with no linearization applied to the meter. It can be observed that there is meter factor variation of the order of 0.7 % in the transition region between 2,000 and 4,000 Re, but that for Reynolds numbers below 2,000 the meter factor is constant within +/- 0.1 %. The implication of the constant meter factor below 2,000 Re is that the velocity profile is not varying significantly in the laminar regime and that the path velocity measurement accuracy does not vary significantly over the range of conditions in this test.

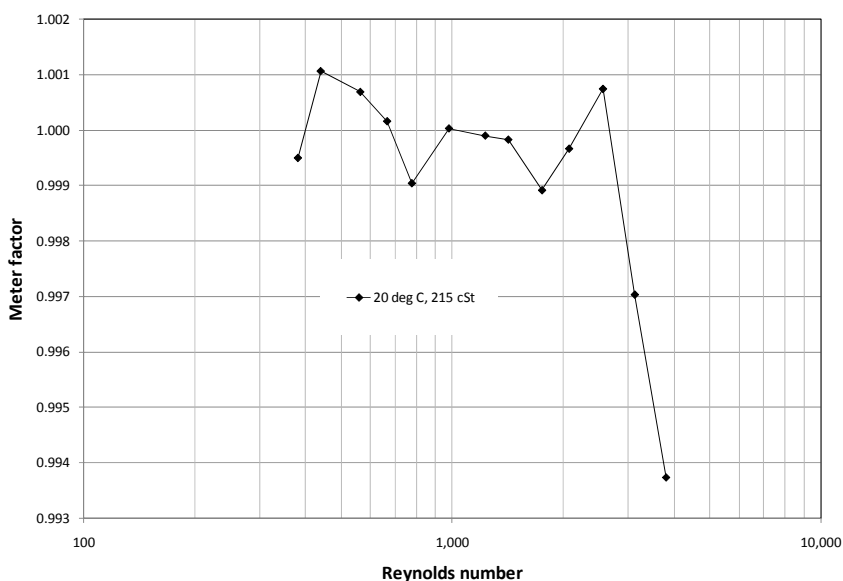


Figure 1 Calibration results for transitional and laminar flow with an oil temperature of 20 °C

Figure 2 below shows the data from Figure 1 with the addition of results obtained using the Primol product at two elevated temperatures of 30 and 45 °C. Also shown on the graph are results from a lower viscosity oil, of 22 cSt at 30 °C, used to obtain further data in the turbulent regime. From this graph it can be observed that there are differences in meter factor of around 0.5 % in the transition region between approximately 3,000 and 5,000 Re, and that in turbulent flow, above 5,000 Re, there is good agreement between the different test conditions. However, what is remarkable is the lack of agreement at Reynolds numbers below 3,000. Taking the data close to 2,000 Re, the meter factor has changed by almost 1.4 % at 30 °C and around 3.5 % at 45 °C.

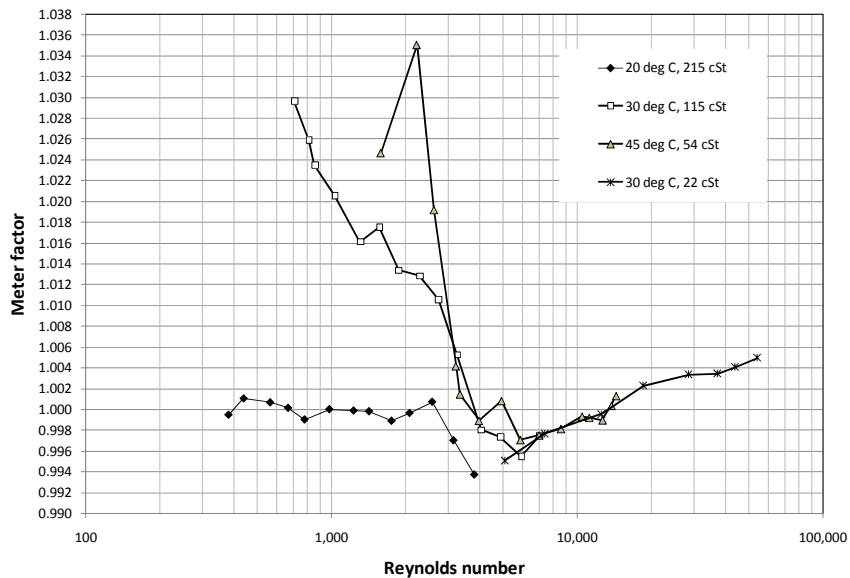


Figure 2 Calibration results showing the effects of oil temperature in the laminar regime

When the results shown in Figure 2 were first obtained, diagnostic data from the meter was scrutinised in an effort to understand what was happening. Parameters related to signal quality, such as gain and signal to noise ratio showed little change over the range of the tests. However, analysis of individual path velocity and sound velocity data produced much more informative results.

Figure 3 below shows the flatness ratio reported by the meter plotted versus Reynolds number for the Primol product at three temperatures. The flatness ratio is calculated by dividing the velocity measured on the two inside path of the 4-path meter (paths 2 and 3) by the velocity on the two outside paths (paths 1 and 4).

This diagnostic analysis clearly shows the transition from laminar to turbulent flow occurring at a Reynolds number of around 3,000. At 20 °C it can be observed that in laminar flow the flatness ratio levels out to a constant value of approximately 0.4 for $Re < 1,000$. However, as the temperature is increased, it can be observed that the flatness reduces, implying that either the velocity profile is changing or that somehow the path velocity measurements are being affected by the change in oil temperature.

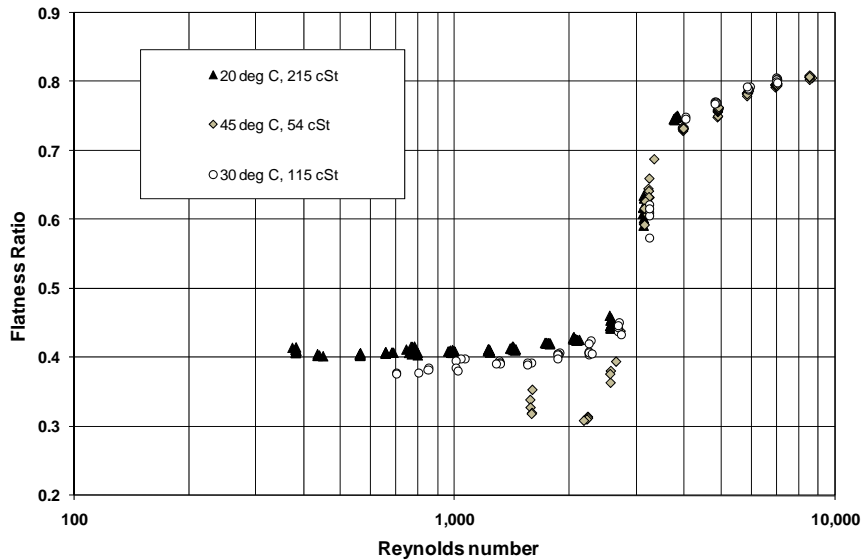


Figure 3 Flatness ratio versus Re at three temperatures

Figure 4 shows the difference between the individual values of sound velocity on each path and the weighted mean average of all four paths. From this graph it is clear that there is good agreement between the sound velocity values above 3,000 Reynolds number at all temperatures and also below 3,000 Reynolds numbers when the oil temperature was 20 °C. However, at 30 and 45 °C the outside paths (paths 1 and 4) register higher sound velocity values than the inside paths, the deviations being most significant on the bottom path, path 4.

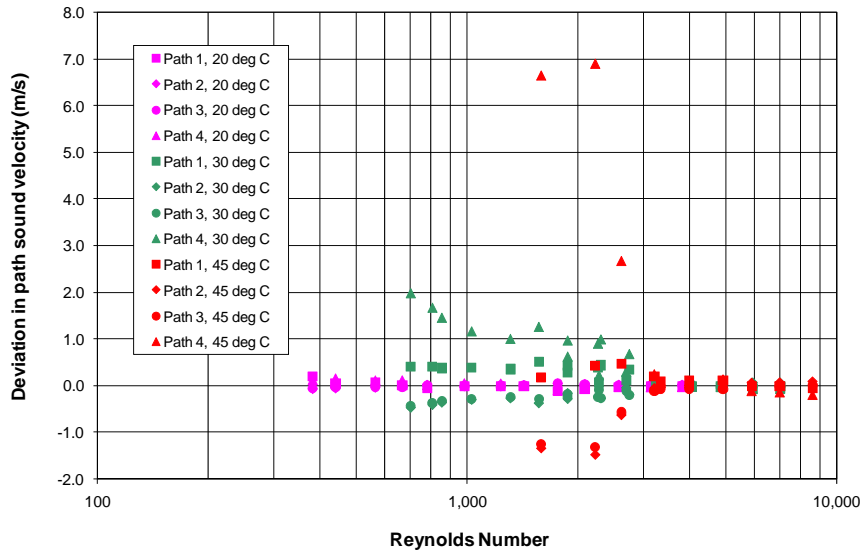


Figure 4 Relative variations in path velocity of sound readings

Taken collectively, the information in Figures 2 – 4 clearly suggest the presence of thermal gradients in laminar flow conditions.

As these results were obtained during the period when the meter design with the integrated reducing nozzle was being developed and tested, results were also obtained using a 6-inch reducing nozzle meter with a 4-inch throat. The results obtained at two temperatures, 20 and 30 °C, are shown in Figure 5 below. At 2,000 Reynolds number, the maximum difference in meter factor at the two conditions is approximately 1.4%.

These results illustrate that the magnitude of effect of the thermal gradients are very similar for the meter with the reducing nozzle and the one without. The reasons for this will be discussed later in the paper.

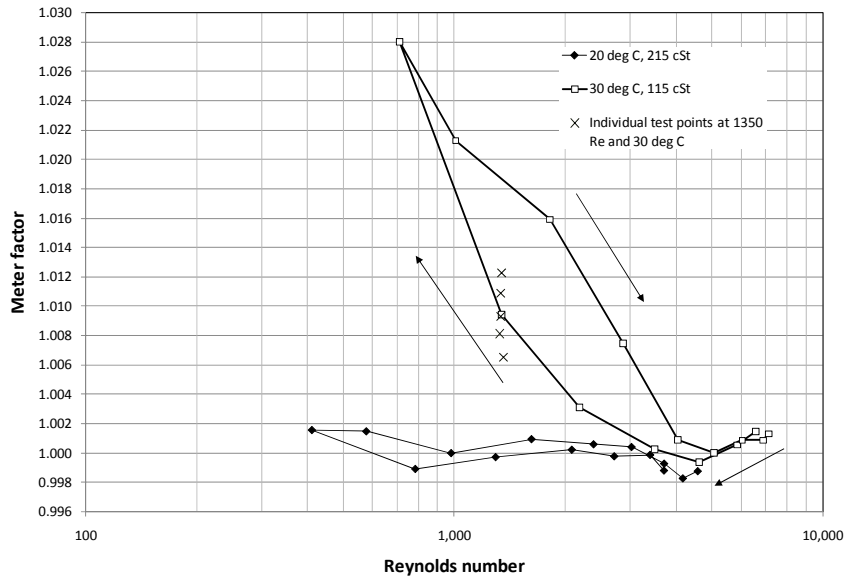


Figure 5 Thermal gradient effect on a reduced bore meter at 30 °C

A further interesting feature of the data in Figure 5, is that there is an apparent 'hysteresis' in the data. This is evidence of a 'thermal time delay' as the whole system reacts to the changing conditions. In Figure 5, the results were obtained in a calibration where the tests started at high Reynolds numbers, progressed down through the Reynolds number range, and then back up again (as illustrated by the arrows). Looking in detail at the test points obtained at 1,350 Reynolds number and 30 °C (shown in Figures 5 and 6) it can be observed that the 'spread' in meter factor at that condition is not in fact a lack of repeatability but a gradual increase in meter factor of more than 0.5% over a period of 15 minutes. This effect will also be discussed further on in the paper.

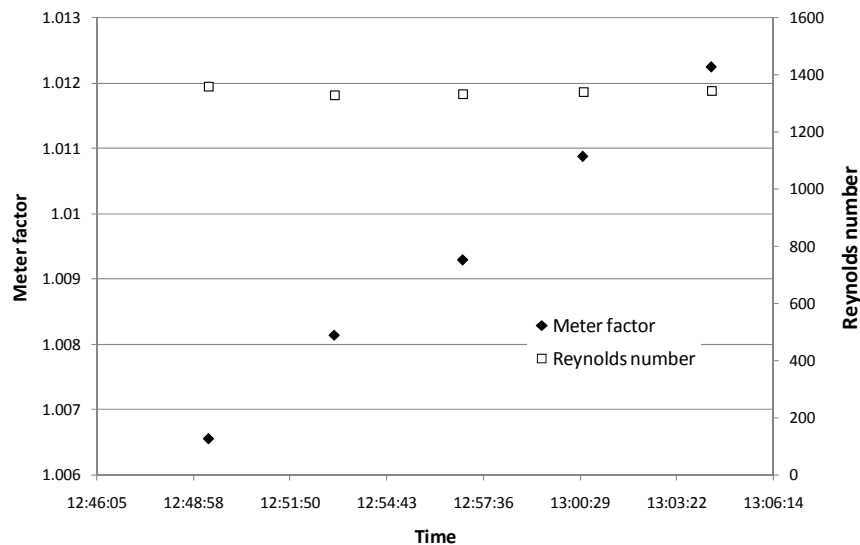


Figure 6 Variation in meter factor as a function of time at 30 °C and 1,350 Re

4 CFD ANALYSIS

After the results described in the previous section had been obtained, it was decided that computational fluid dynamics should be used to give some more insight into the problem.

The CFD modelling described here was carried out for Cameron by Neil Barton of NEL.

Flow was modelled in a straight pipe of 6-inch diameter, 200 diameters long. The oil temperature at the inlet to the pipe was set at 30 °C, and the density and viscosity properties of the oil versus temperature were matched to the Primol test oil (approx 860 kg/m³ and 115 cSt at 30 °C). The simulation flowrate was set to approximately 23 kg/s, such that the resulting Reynolds number at the inlet would be close to 2,000. Further details are given in the NEL report [7].

Two different cases of heat loss were modelled. In the first case the pipe wall was cooled by convective heat loss, with the surrounding air temperature set to 20 °C. In the second case the temperature of the pipe wall was set to 20 °C. This second case represents a very extreme situation, which is highly exaggerated with respect to what is likely in practice (unless of course the differential between ambient and oil temperature is much much higher).

There are some differences in scope between the CFD analysis carried out by NEL and that described by Hogendoorn et al [6], as outlined in the table below. However, as will be shown these differences are not believed to have a significant impact on the general conclusions that can be drawn from the CFD analysis.

	NEL/Cameron	Hogendoorn et al
Temperature differentials	Case 1 – convective heat loss, fluid: 30 °C, ambient: 20°C Case 2 – fluid: 30°C, pipe wall: 20°C	Fluid: 35 °C Pipe wall: 15, 30, 35, 40 and 55 °C
Buoyancy effects included	Yes	No
Viscosity at 20 deg C	215 cSt	400 cSt
Reynolds numbers	2000	100, 500, 1500
Pipe diameter	6-inch	4-inch
Downstream location of meter	From 5 – 200 D, in 5 D steps	50 D
Meter design	4-path, full bore	5-path, reduced bore

Figure 7 below shows colour plots of the temperature distribution inside the pipe at 200 diameters downstream. The effects of buoyancy are apparent in both plots. In the left hand figure, the convective heat loss creates a 'hot spot' at the top of the pipe where the heated air is rising from around the pipe. In the right hand plot, the higher density of the cooled liquid tends to lead to stratification at the bottom of the pipe. It should be noted that the colour scales are different on the two temperature plots, the span being 10 °C in the right hand plot and only 1.4 °C in the left hand plot.

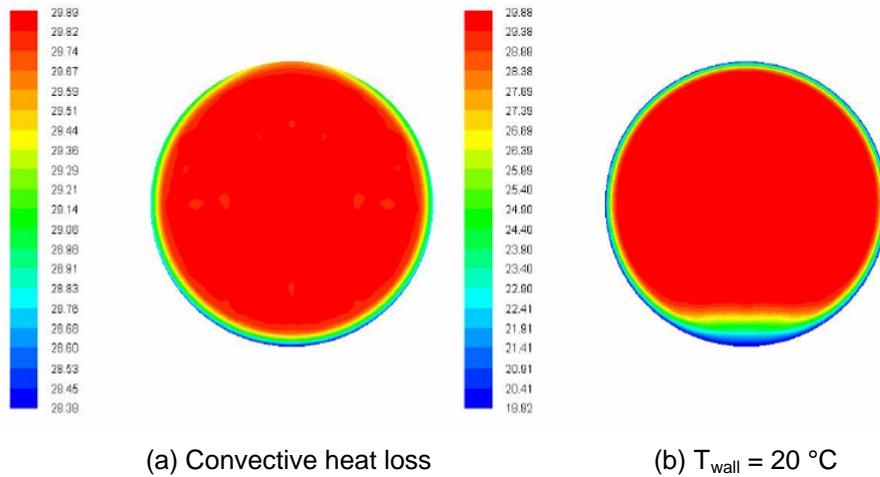


Figure 7 Temperature contours at 200 diameters downstream

Figure 8 shows velocity profile colour contour plots at 200 D downstream. In each case the image is split in two, with the left hand half showing fully developed laminar flow and the right hand half showing the velocity profile for each thermal condition that has been modelled. From these images it is clear that there has been relatively little effect on the velocity profile in the convective heat loss case. In the case of the wall temperature set at 20 °C, the most obvious effect is the reduction in velocity towards the bottom of the pipe.

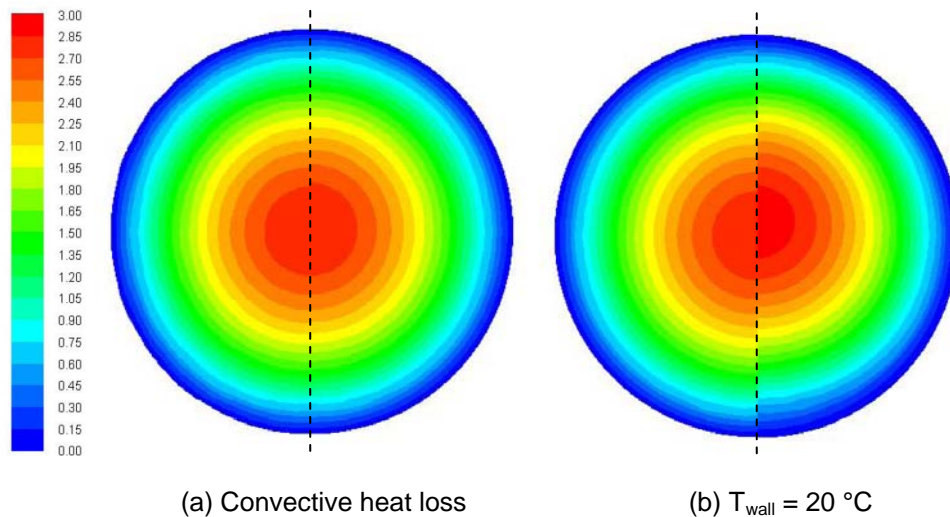


Figure 8 Velocity profile contours at 200 diameters downstream

Figure 9 shows the results of integrating the velocity profiles according to the design of a 4-path Gauss-Jacobi meter design, for each of the heat transfer cases, and comparing that with the results from fully developed laminar flow. It can be observed that in the case of convective heat loss, there is very little influence on the meter, with the shift reaching a maximum of about -0.025 % at 200 D. In the more extreme case where the wall temperature was set to 20 °C, the shift tends to a maximum of around -0.2 % at around 100 D. Note that the 'spikes' in the CFD results do not represent what is happening physically, but are a result of uncertainties in the modelling process.

Whilst we have to recognise that there are differences between this CFD work and that of Hoogendorn et al, the broad conclusion that can be drawn from both studies is that the changes in velocity profile due to thermal gradients should not affect the calibration of multipath ultrasonic meters by more than a few tenths of a percent. The question then is: what is the cause of the differences observed in the test results that are an order of magnitude greater?

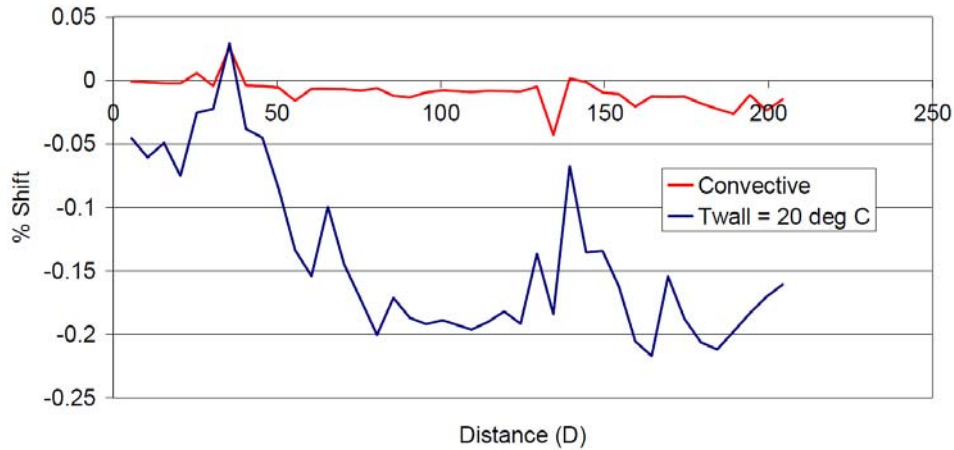


Figure 9 Simulation of the temperature related velocity profile effects on a 4-path meter

5 A MECHANISM FOR THE EFFECTS OF THERMAL GRADIENTS

With the benefit of hindsight, the cause of the large differences in meter factor that occur when thermal gradients are present is rather obvious. The geometry assumed for the paths of an ultrasonic meter connect the transducer centres along a straight line, with a particular angle to the pipe axis. When thermal gradients are present, this is no longer true, as the ultrasound undergoes refraction as it passes through the sound velocity gradient that is also present as a consequence of the temperature gradient.

Consider what happens when the thermal gradient is present inside the meter body itself. In laminar conditions, the fluid in the recesses or cavities in front of the transducer housings is trapped and is either stagnant (at very low Re) or recirculated within the cavity. As such it will eventually take on the temperature of the oil closest to the pipe wall. The result (in the case of hot oil and a cooler ambient temperature) is that the ultrasound must pass from a region of higher sound velocity to a region of lower sound velocity.

With reference to Figure 10 below, Snell's law of refraction for acoustic waves can be written as

$$\frac{\cos \theta_i}{c_i} = \text{constant} = \frac{\cos \theta_1}{c_1} = \frac{\cos \theta_2}{c_2} = \frac{\cos \theta_3}{c_3} = \frac{\cos \theta_4}{c_4} \dots$$

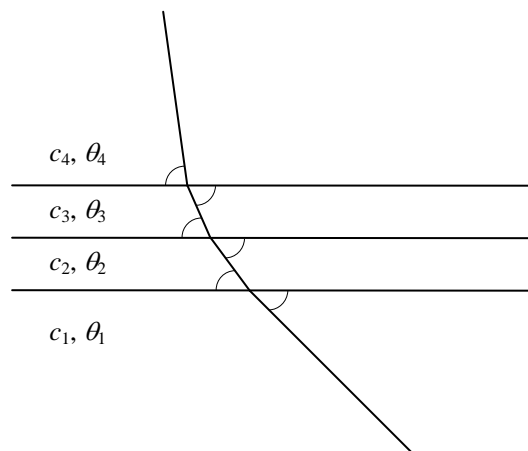


Figure 10 An illustration of Snell's law of Refraction

What this relationship shows is that owing to the transducer face being at an angle to the pipe axis (typically 45°), it must undergo refraction as it passes through the thermal gradient, which will be roughly parallel with the pipe wall. Snell's law also illustrates that is not important that the change in velocity of sound occurs as a gradient rather than a sudden change, the overall change in angle is only dependent on the sound velocity on either side of the layer.

In reality the effects are quite complex, particularly when the three-dimensional geometry of the transducer cavities are considered, as pictured in Figure 11. The refraction effect means that the effective location of the path with change both in terms of its angle to the pipe axis, and its lateral offset (height) in the cross section.



Figure 11 A photograph showing the complex geometry of a transducer cavity

In order to illustrate the effect with a very simple example, consider an ultrasonic wave that meets a change in sound velocity at an angle of 45°. If the sound velocity on the 'cold' side the interface is 1441 m/s and on the 'warm' side it is 1434 m/s, then the path angle would change by approximately 0.3°. While this might not appear to be a large change in angle, corresponding change in the transit time difference would be almost 1%.

The values of sound velocity in the above example correspond to a change of roughly 2 °C in oil temperature. This illustrates that refraction is a physical mechanism that can easily explain effects of the magnitude seen in the experimental data.

Understanding that it is the mechanism of refraction that is responsible for meter factor changes in laminar flow also explains why the meter design with the reducing nozzle has a response that is very similar to the full-bore meter. Although the thermal boundary layer will be 'squeezed' as it goes through the reducer, ultrasound still has to pass from one side of the layer to the other, and the effects of refraction will be virtually the same.

The refraction mechanism also explains the thermal time delay effects shown in Figures 5 and 6. Consider that in turbulent flow the fluid is well mixed and the temperature is the same in the transducer cavities and in the bulk flow. If the ambient temperature is lower than the oil temperature when the flow then drops into laminar conditions, the fluid closest to the pipe wall begins to cool (and also flows downstream). This creates a layer of cool oil that encloses the fluid in the transducer cavity. It then takes some time for the thermal boundary layer to thicken and fluid trapped in the cavity to cool to the outside temperature of the boundary layer, by which time the refraction effect reaches its maximum.

6 CONDITIONS AFFECTING THE DEVELOPMENT OF THERMAL GRADIENTS

The data in Figure 9 above shows that thermal gradients develop gradually downstream of a point of where the fluid is isothermal. In practice this means that if the meter is a short distance from this point, or if there is repeated mixing of the fluid, then the effects on the meter may be less significant. So in some applications significant thermal gradients may develop and in others they may not. At present it is not easy to judge when thermal gradients will be a problem or not, as it is dependent on many factors including the pipe geometry, the fluid and ambient temperatures, the meter design, and potentially other factors such as velocity or Froude number.

Figure 12 shows results from a 12-inch meter with reducing nozzle tested at NEL over a range of temperatures [2]. Based on the earlier results shown in Figure 5, it might be expected that at the lowest Reynolds numbers in this test (below 3,000 Re), there would be some evidence of the detrimental effects of thermal gradients. However, in this case there was only a slight suggestion of thermal gradients in the diagnostic data. In all probability the lack of effects in this case was due to the fact that there was only a relatively short length of around 20 diameters of 12-inch pipe upstream and prior to that the flow came through an complex series of combining and dividing flow and bends, all in 8-inch diameter.

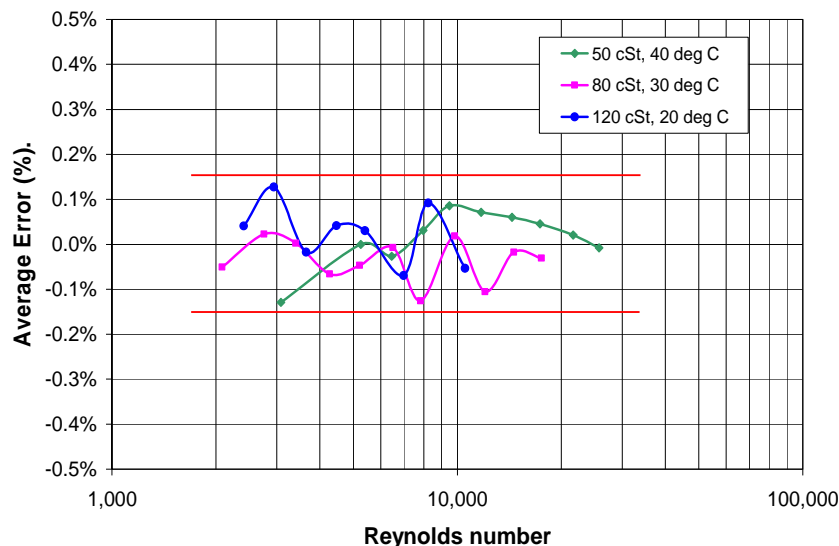


Figure 12 An example of calibration results absent of the effects of thermal gradients

Figure 13 on the other hand shows data for a 12-inch meter calibrated at SPSE in France under two different sets of conditions. The test lines are outside at SPSE and the tests were conducted in the months of December and January with the result that the ambient temperatures were low. Two different oils were used and in one instance the oil temperature was in the range of 10 – 17 °C, and in the other case the oil temperature was in the range of 28 to 35 °C. The data at Reynolds numbers between 4,000 and 6,000, showed a lack of reproducibility and clear evidence of the effects thermal gradients in the diagnostic data. This case is interesting as the line set up at SPSE is quite similar to many metering installations, comprising a header upstream of two parallel test lines.

Although laminar flow would not normally be expected at the relatively high Reynolds numbers shown in Figure 13, the meter diagnostics such as the flatness ratio clearly showed that the flow was laminar below 4,000 Re. In this case it appears that the heat transfer is also playing a part in where the transition occurs. It is stated by Schlichting that “the transfer of heat from the boundary layer to the wall exerts a stabilising influence by causing the critical Reynolds number to increase” [4], i.e. transition and hence laminar flow can occur at higher Reynolds numbers when heat loss through the pipe wall is present.

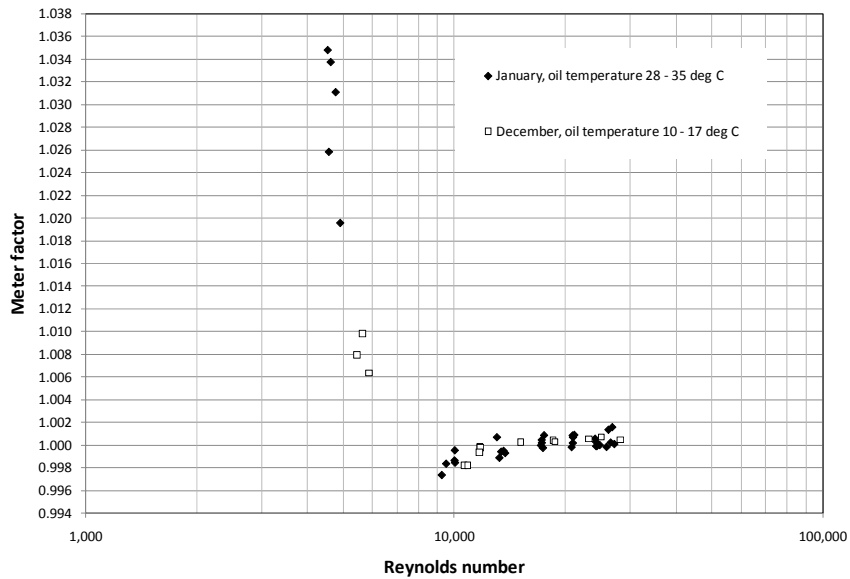


Figure 13 Thermal gradient effects observed during calibrations at SPSE

7 REDUCING THE IMPACT OF THERMAL GRADIENTS

7.1 Experimentation

Given the understanding that the effects observed experimentally are a result of thermal gradients and the resulting refraction of the ultrasonic beams, the question then is find ways to reduce or correct for these effects. This is an area in which Cameron have carried out a considerable amount of experimental work in recent years.

Initial experiments were designed to investigate various effects included testing meters with paths vertical rather than horizontal, testing with insulation over part of the installation, and testing with various conventional flow conditioners and mixers. A sample of the results of these tests are presented below.

Paths orientated vertically

Given that the experimental results showed evidence of buoyancy effects/stratification, a test was conducted where the flowmeters were reorientated such that their paths were vertical rather than horizontal. The tests were conducted without insulation or flow conditioning and the results for the two orientations compared under nominally identical test conditions. The results are shown in Figure 14 below for a 6-inch full-bore Caldon 240C ultrasonic meter. It can be observed that orientating the paths vertically produces virtually the same results in terms of the effect of temperature on the meter factor. This is due to the fact that the thermal boundary layer extends around the entire internal circumference of the pipe.

Similar results to those shown in Figure 14 were also obtained when the same test was performed on the meter design with reducing nozzle.

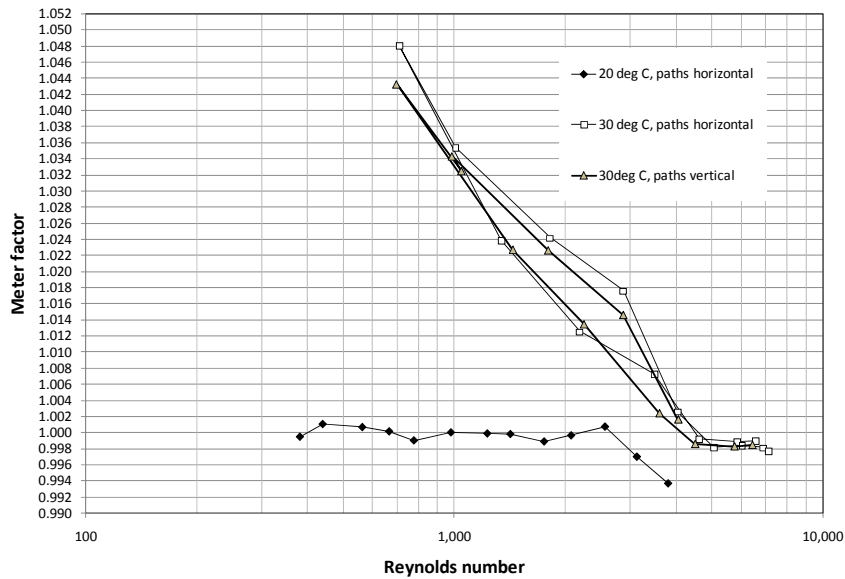


Figure 14 Results obtained with paths horizontal and vertical

Meter body and 20 diameters of pipe insulated

An obvious question to ask is: what is the effect of applying insulation to the upstream pipe and meter body? To answer this question a test was performed with approximately 70 diameters of straight pipe in total upstream, with 150mm glass mineral wool insulation applied to 20 diameters upstream of the meter and the meter itself.

The results are shown in Figure 15 below, for a meter of the reducing nozzle design (6-inch meter with a 4-inch throat). In this case the insulation was found to have a beneficial effect, reducing the overall magnitude of meter factor variability.

However, the insulation was certainly not 100 % effective. This can be explained if we consider what insulation can and cannot do. It can minimise heat transfer between the pipe wall and the outside environment, but it cannot prevent heat transfer to or from the fluid itself. If the pipe wall is at the fluid temperature in turbulent flow, then when the flow changes to a laminar condition the uninsulated pipe will begin to cool. The cool boundary layer will flow downstream into the uninsulated section and will itself have a cooling effect on the pipe wall and meter body under the insulation. In fact, it is possible to imagine that given sufficient time the temperature under the insulation could equalise with the temperature of the exposed pipe.

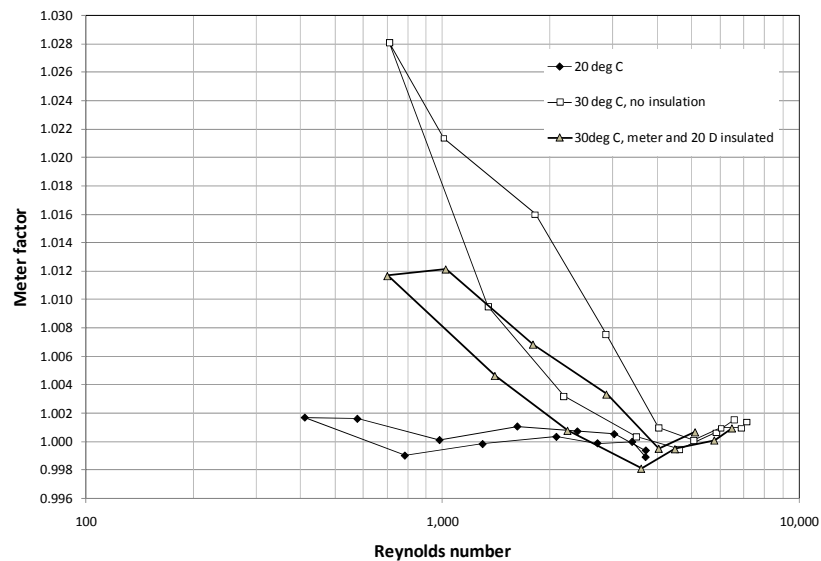


Figure 15 Results obtained with and without insulation

Tests with a Spearman perforated plate flow conditioner

Tests were carried out with various conventional forms of flow conditioning and mixing devices. Encouraging results were sometimes obtained by using two different devices in series, for example a mixer followed by a flow conditioner, but with the penalty of high pressure loss. Of the conventional flow conditioners, one which produced a fair degree of improvement on its own was a Spearman perforated plate. The plate was used at various distances from the meter, with similar results being obtained with the conditioner at distances of between 3 and 10 diameters upstream of the meter.

Figure 16 shows the results of tests with the Spearman plate just 3 diameters upstream of a meter with reducing nozzle, again with oil temperatures of 20 and 30 °C. It can be observed that the results are in very close agreement down to a Reynolds number of around 3,000 and then there is some divergence. However, at a Reynolds number of 1,000, the difference in variation is meter factor is only about 0.5 %, as opposed to more than 2 % for the same meter with no flow conditioning.

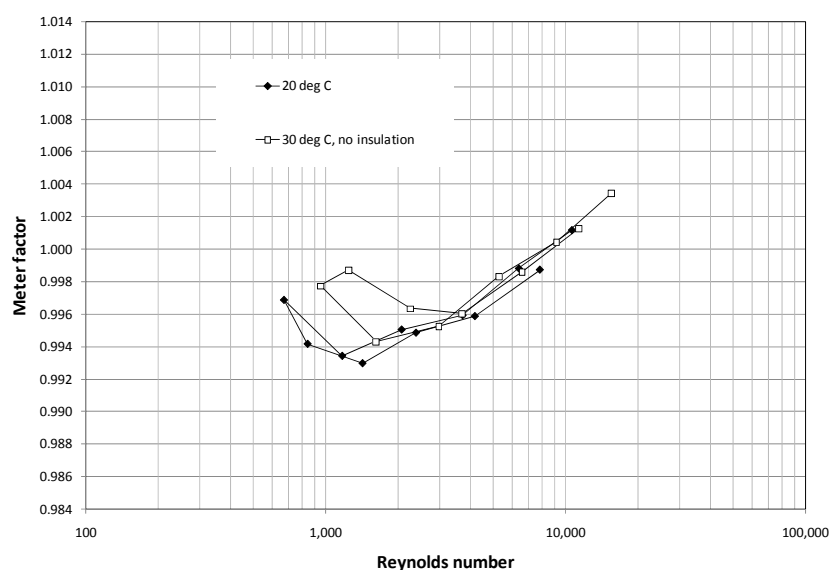


Figure 15 Results obtained with the Spearman plate for 20 and 30 °C

In general it was true of the flow conditioning devices tested that improvements were made but that below 1,000 Reynolds number the uncertainty tended to exceed the bounds required for custody transfer.

Empirical corrections applied in the meter

Analysis of various data sets showed that a meter could be calibrated or 'tuned' to reduce the effects of thermal gradients over a range of test conditions. However, the basis of such corrections is empirical and as such the applicability of the corrections outside of the specific calibration conditions would be questionable. For that reason it was deemed preferable to pursue a flow conditioning based solution.

7.2 Development of a New Design of Flow Conditioner

Following the period of experimentation described above, consideration was given to the design of a flow conditioner that would address the specific problem of thermal gradients in laminar flow. Various ideas were reviewed and then discarded as either as being ineffective or impractical. Eventually the idea was put forward of a device that would use ramps to direct the thermal boundary layer away from the pipe wall, whilst simultaneously directing fluid from beyond the boundary layer towards the pipe wall to replace the fluid displaced from there. A practical design based on alternating ramps extending from a tubular body of diameter smaller than the pipe internal diameter was then devised.

The photograph in Figure 17 shows a prototype of the 'laminar boundary layer flow conditioner' that comprises two sets of ramps in series, providing additional displacement and mixing of the fluid close to the pipe wall. This is the device that was used to obtain the test results described below.

The prototype laminar flow conditioner was tested at NEL using their Paraflex oil. The meter used in the test was a 6-inch 8-path full bore meter installed with approximately 80 diameters of straight pipe upstream. For the first set of tests the flow conditioner was not installed and the upstream pipe and flow meter were not insulated. For the second set of tests, the conditioner was installed 10 diameters upstream of the meter, and the upstream pipe was insulated with 150 mm glass mineral wool wrapped round the pipe from the mixer element to the meter, and including the meter itself. The purpose of the insulation was to prevent redevelopment of thermal gradients between the conditioner and the meter.

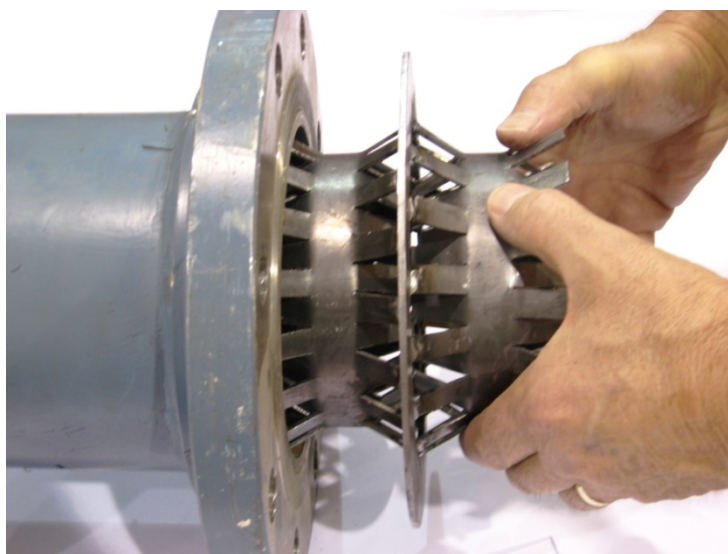


Figure 17 A photograph of the prototype laminar boundary layer flow conditioner

The two graphs shown below summarise the performance in terms of meter factor versus Reynolds number for the meter through laminar, transitional and turbulent flow, with and without the mixing device.

Figure 18 shows the behaviour of the meter without the flow conditioner in the line. This data is presented with no linearization applied in the meter. It can be observed that below around 3,000 Re, the calibration curves diverge as a function of temperature. It can also be observed that hysteresis is observed before below 3,000 Re, particularly at the elevated temperatures. As discussed earlier, the hysteresis is caused by the system not being at thermal equilibrium, and therefore meter factors change progressively over time as the fluid close to the pipewall and in the transducer cavities either heats or cools.

It can be observed that without the mixer the deviation between the 20 °C condition and the 40 °C condition at 800 Re, is approximately 2.7%.

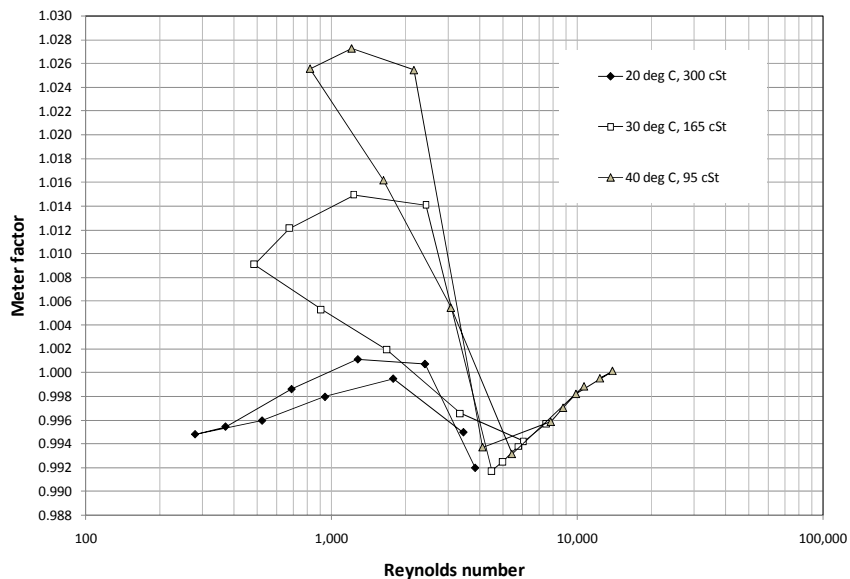


Figure 18 Full-bore 6-inch 8-path meter without flow conditioner (raw meter factor)

Figure 19 below shows the performance with the flow conditioning device installed 10 diameters upstream, and with the meter and pipework between insulated. This data is also presented with no linearization applied in the meter. It can be observed that the line of the turbulent flow meter factor now continues down to around 2,500 Reynolds number, where transitional behaviour was previously seen between 3,000 and 4,000 Re. As might be expected with a full bore meter design, there is a sharp change in meter factor in the transition between laminar and turbulent flow centred at around 2,000 Re. In applications that span the transition, this sudden change can be smoothed out by use of a reducing nozzle [2].

The benefits of the flow conditioning device can be observed in the improved reproducibility of the meter factor in the laminar region below 2000 Re. It can be seen that the maximum deviation in that region is now within +/- 0.15 %, i.e. there is an order of magnitude improvement. It is also useful to note, that above 5,000 Re, in the turbulent regime, the meter factor has the same value with and without the flow conditioner.

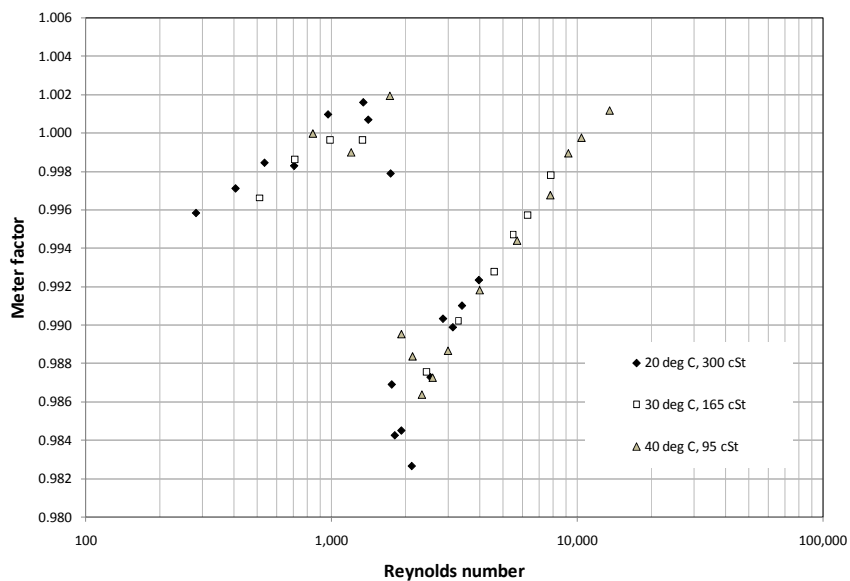


Figure 19 Full-bore 6-inch 8-path meter with laminar flow conditioner (raw meter factor)

The results shown in Figures 18 and 19 demonstrate that this conditioner has been effective at reducing the effects of thermal gradients to a sufficiently low for level custody transfer applications. Preliminary analysis shows that this improved benefit is obtained with significantly lower pressure loss than for a perforated plate conditioner. Further work is still required to optimise the design both in terms of its effectiveness and its pressure drop.

8 DISCUSSION AND CONCLUSIONS

The experimental data presented in this paper clearly demonstrates that thermal gradients in laminar flow can have significant effects on the performance of ultrasonic flow meters. The possibility of thermal gradients being present in the flow arises whenever the flow is laminar and there is a differential between the fluid and ambient temperatures.

The use of a meter design incorporating a reducing nozzle or convergent section is beneficial in terms of transitional flow and the generally ability to cope with higher viscosities but does not help to reduce the impact of thermal gradients.

The primary mechanism by which thermal gradients affect the performance of ultrasonic meters is not velocity profile, it is refraction, resulting from the fact that the ultrasonic paths must cross a sound velocity gradient.

CFD analysis has proven to be a useful tool for aiding understanding of the formation of thermal gradients, but has not been effective in predicting their effect on ultrasonic meters, owing to the fact that the effects of refraction have not been accounted for in the modelling process.

In practice the severity of thermal gradients, and hence the resulting effects on ultrasonic meters will be a function of many variables including:

- Oil properties
- Reynolds number and velocity
- Pipe diameter
- Fluid and ambient temperatures
- The quality and extent of insulation
- The effects of the upstream pipe configuration, including bends, flow conditioners, pumps and valves

It has been shown that insulating the pipe upstream of a meter can have beneficial effects, but is not sufficient to ensure custody transfer levels of uncertainty if thermal gradients are established in the pipe upstream of the insulation.

It has also been demonstrated that use of a perforated plate flow conditioner can reduce the impact of thermal gradients, but that at lower Reynolds number in the laminar regime, the effect on the meter factor can still be significant.

Tests of a prototype laminar boundary layer flow conditioner have demonstrated that it is effective in reducing the effects of thermal gradients to level consistent with the requirements for custody transfer. Even before the prototype has been optimised, this benefit is achieved with lower pressure loss than a conventional perforated plate flow conditioner.

REFERENCES

- [1] Fronek, V (1978) *Ultrasonic measurements of oil flow in a laminar flow-turbulent flow transition region* Proceedings of FLOMEKO '78, Groningen, The Netherlands, 11-15 September 1978, H H Dijstelbergen & E A Spencer (eds), North-Holland Publishing Co, Amsterdam, pp. 141-146.
- [2] Brown, G J, Cousins, T, Augenstein, D R and Estrada, H (2009) *A multipath ultrasonic meter with reducing nozzle for improved performance in the laminar/turbulent transition region*, North Sea Flow Measurement Workshop, Tonsberg, Norway.
- [3] Miller, D S (1990) *Internal Flow Systems*, 2nd Edition, BHRA, Bedford.
- [4] Schlichting, H (1968) *Boundary Layer Theory*, McGraw-Hill, New York
- [5] http://www.oil-transport.info/Crude_oil_data/crude_oil_data.html
- [6] Jankees Hogendoorn, J, Tawackolian, K, Van Brakel, P, Van Klooster, J, and Drenthen, J (2009) *High viscosity hydrocarbon flow measurement, a challenge for ultrasonic flow meters?*, North Sea Flow Measurement Workshop, Tonsberg, Norway.
- [7] Barton, N (2007) *CFD simulation of temperature effects on an ultrasonic flowmeter*, NEL Report No 2007/126

Paper 6.2

Field Comparison of a Mechanical and Electronic Custody Measurement Loop for Hydrocarbon Liquids

Mohammed Salim
Saudi Arabian Oil Company (Aramco)

Ibrahim M. Al-Qahtani
Saudi Arabian Oil Company (Aramco)

Yousef A. Al-Jarallah
Saudi Arabian Oil Company (Aramco)

Waleed A. Al-Shaya
Saudi Arabian Oil Company (Aramco)

Ali A. Haddad
Saudi Arabian Oil Company (Aramco)

Field Comparison of a Mechanical and Electronic Custody Measurement Loop for Hydrocarbon Liquids

Dr. Mohammed Salim, Saudi Arabian Oil Company (Aramco)
Ibrahim M. Al-Qahtani, Saudi Arabian Oil Company (Aramco)
Yousef A. Al-Jarallah, Saudi Arabian Oil Company (Aramco)
Waleed A. Al-Shaya, Saudi Arabian Oil Company (Aramco)
Ali A. Haddad, Saudi Arabian Oil Company (Aramco)

1 INTRODUCTION

Metering systems typically use turbine meter(s) and a prover as the primary source of measurement. Both the turbine meter and the prover are mechanical devices – mechanical loop. The performance of a turbine meter changes under various operating conditions and requires regular calibration using a prover for maintaining the accuracy. Mechanical loops are also prone to frequent failures during their life cycle. If the mechanical loop can be redesigned using the ultrasonic meters in a meter/prover combination (master metering) significant improvement can be realized in the operation and maintenance of these critical systems. The main concern is if the electronic loop can provide the same or better level of measurement accuracy while retaining the same repeatability, reproducibility, etc., of the presently accepted mechanical loop.

A number of tests have been conducted on the ultrasonic meter technology for liquids using various configurations and sizes of meters [1], [2], [3], [4], however, the authors have not found any published literature where this technology has been tested in not only comparing directly against the conventional metering system design (mechanical loop), but also the master metering using ultrasonic meters (electronic loop) within the same system with synchronized batching and proving. This type of configuration allows for various types of comparisons to be made with the 2 loops – proving a meter using the conventional prover and master metering using the ultrasonic meter to determine the meter factor, etc.

The field setup is comprised of a 20-inch turbine meter, two 20-inch ultrasonic meters and a 42-inch prover. The control system include each meter having its own flow computer with supervisory integrating the measurement functions for synchronized testing.

This paper discusses the system design and compares test results between a conventional custody metering system design (mechanical loop) and an electronic master metering loop. The mechanical and electronic loops were designed in the same system and tested with synchronized batching and proving to allow direct comparison of the conventional loop and master metering (ultrasonic as master) with ultrasonic to ultrasonic and ultrasonic to turbine meter. This design enables testing of all the meters within a closed loop along with a prover being subjected to the same operating conditions and synchronized in performing the measurement functions.

2 PHASE 1 TESTING OF ULTRASONIC METER

Initial tests conducted on this technology were with a turbine and a single ultrasonic meter connected to an online prover. The setup was designed to perform synchronized batching and proving. The control signals for starting and ending batches and proving was with the turbine meter/prover loop. The ultrasonic meter performed its tasks through activation signals from the turbine/prover metering control system.

Fig.1 provides the basic layout arrangement of measurement system setup used in phase 1. The test was performed at one of Saudi Aramco's operational facilities. Modifications to existing meter streams in the field and the metering control system were done to setup the test system. A separate test measurement system was developed to capture the data; however, master metering had to be activated manually in the test measurement system.

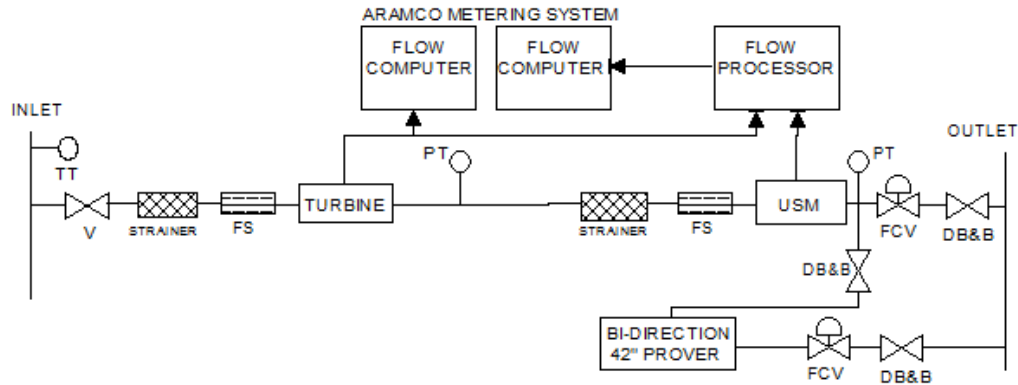


Fig. 1 Measurement system setup for phase 1 test

The primary purpose of the test was to verify the vendor's claims for this technology, in particular:

- Viscosity independent (no need for multi-product calibration)
- No need for frequent calibration
- High accuracy, repeatability and reliability
- Low pumping costs
- Low maintenance costs

If the above can be achieved, this technology would certainly improve some aspect of the widely accepted mechanical loop.

2.1 Viscosity Independent Test

The meter was tested with four types of crude (Arabian Light, Arabian Extra Light, Arabian Medium, and Arabian Heavy). The API range for these crudes is from 26.5 – 38 with a viscosity of 41 – 230 Centistokes at 70 Deg F.

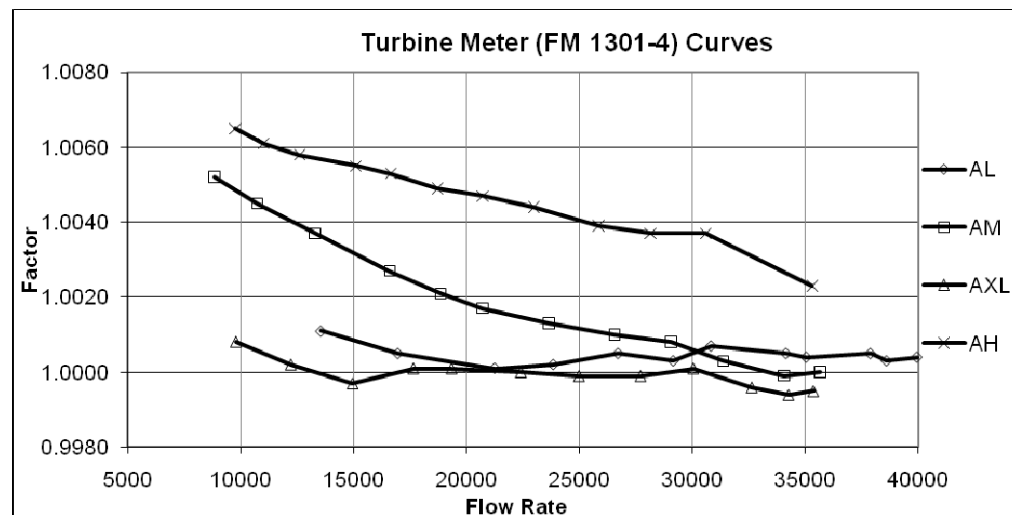


Fig. 2 Turbine meter calibration curves using online prover

Fig. 2 shows the calibration results of the turbine meter for the four types of crude oils. It can be seen from Fig. 2 the turbine meter shows variation in its performance with the different types of crude oils.

Fig. 3 shows the calibration results for the ultrasonic meter for the four types of crude oils.

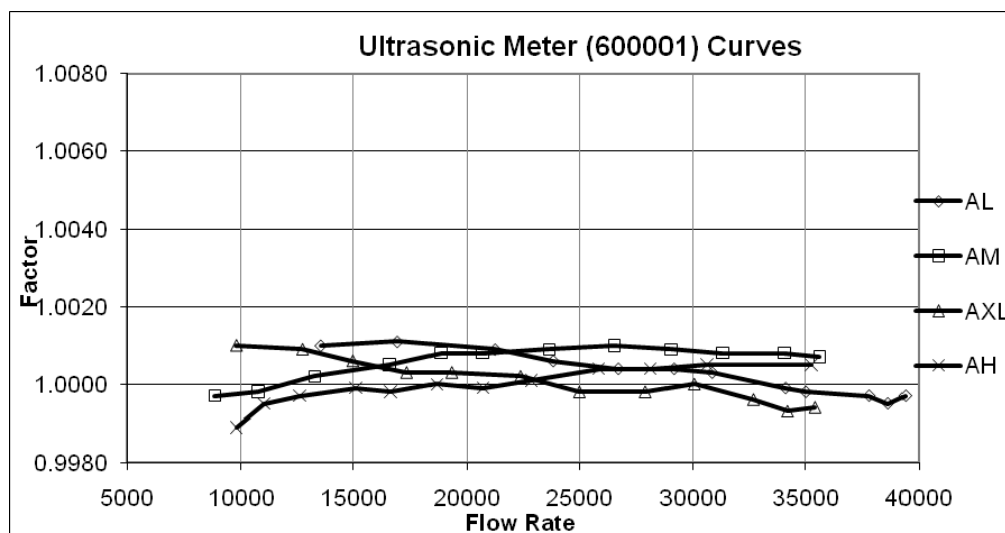


Fig. 3 Ultrasonic meter calibration using online prover

Comparing the results of Fig. 2 and Fig. 3, It can be seen that while the dispersion in the curves for the ultrasonic meter are less than the turbine meter, it cannot be stated that the meter's performance is exactly the same for all types of crude oils. This is after the ultrasonic meter was calibrated for the range of crudes to be measured at a calibration facility.

This test, which was repeated three times during the testing period of about two years for phase 1, shows that the ultrasonic meter will need to be calibrated for the types of liquid to be measured on-site. This is certainly the case found for Arabian crude oils.

2.2 No Need for Frequent Calibration

The most important aspect of the measurement process to which this technology can make a major contribution is in alleviating the frequent calibration of the primary sensor. The turbine meter works happily for several years as long as it is proved continuously for maintaining the accuracy in measurement. There are facilities with large number of meters for the custody transfer measurement; the prover can be used several times a day. The prover being a mechanical device is prone to failure demanding major operational effort to repair and bring back to service. The repair of such devices can take weeks/months depending on the type of failure. This is one of the major setbacks for this widely accepted turbine/prover measurement loop.

If the ultrasonic meter can provide the same or better levels of accuracy, reproducibility, repeatability and reliability, the frequent use of the prover can be reduced.

As the turbine and the prover loop is an acceptable worldwide standard, it is reasonable to use it as a reference in comparing it against any new technology which is looking to replace it. Tests to verify this aspect compared:

- Turbine/prover standard volume (GSV) with USM ISV
- Turbine/prover standard volume (GSV) with USM GSV using historical curve
- Turbine/prover gross standard volume (GSV) with USM GSV online proving

The first option is basically testing the idea that once the ultrasonic meter is calibrated at a calibration agency, there is no need for any further calibration. It will perform accurate measurement without the need for any reference prover to correct the meter performance. The first option failed to satisfy, based on results from Section 2.1.

The second option is basically to have the meter calibrated using a reference prover to develop a correction curve for each liquid being measured. The ultrasonic meter is then used only relying on this historical curve without the need for online prover correction.

If this second option could satisfy, this would imply the meter can be used without having an online prover or if the online prover was necessary then maybe reducing its frequent use.

Fig. 4 shows the results obtained using this comparison. It can be seen that the ultrasonic meter came very close in measurement to the turbine/prover loop when using only the historical calibration curve.

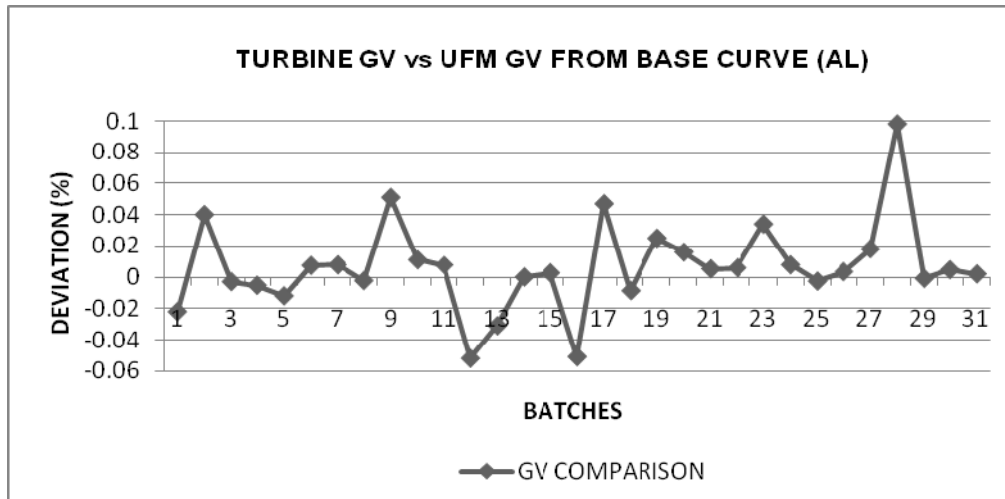


Fig. 4 Turbine/Prover GSV compared with USM GSV using base curve

While there was insufficient data and a point which is questionable, in the main the results provided some confidence in continuing the testing on this technology.

The third option was to use the ultrasonic meter as a direct replacement of the turbine meter in the mechanical loop keeping the prover. The third option has been approved in the API Chapter 5.8 [5].

The repeatability, reproducibility and reliability factor for the measurement process has to be tested.

2.3 Repeatability during Proving of the USM

There have been concerns on the repeatability requirement when proving this meter to generate a meter factor. API Chapter 5.8 [5] provides guidelines on meter size, prover volume, number of runs and repeatability criteria. While API has not stated the meter size and volume used in this test, Fig. 5 shows good results during phase 1 testing.

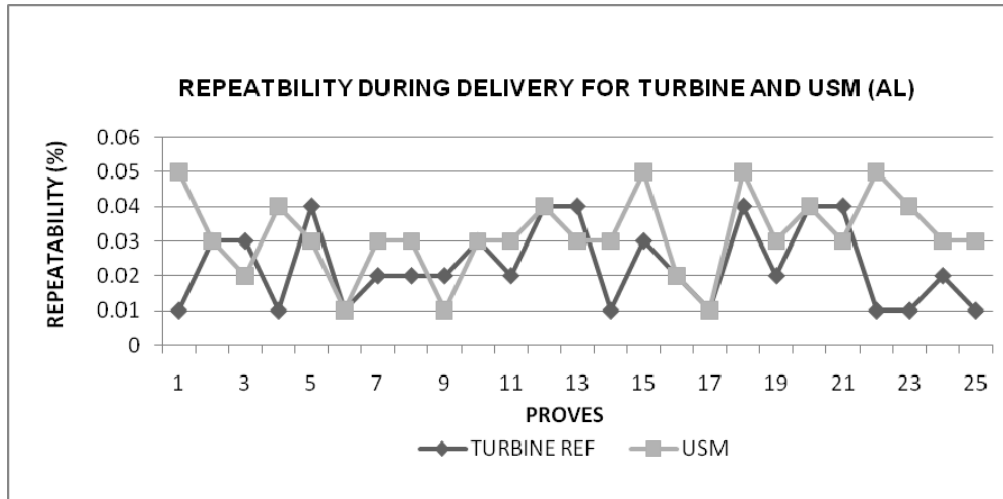


Fig. 5 Repeatability of the meters when proving with an online prover

3 PHASE 2 TESTING OF ULTRASONIC METER

Phase 1 testing provided some encouraging results prompting the continuation of testing the ultrasonic meter; however, there was a need to expand the types of tests to be performed in phase 2. Further tests needed to be performed to see the possibility of reducing the frequent use of the prover in the transfer process. This would imply reducing the usage of the prover, but remaining online. The ideal scenario would be to remove the prover from online to a centralized location. The ultrasonic meters can be calibrated using this centralized prover to develop performance curves for each liquid to be measured based on option 2 of Section 2.2. However for such a scenario, there is a need to check if the meters on duty continue to perform accurately. This can be achieved by having a check meter (master metering) using a second ultrasonic meter in a master/duty arrangement with both meters calibrated against the same reference.

The phase 2 testing will still require batching and proving to be performed using the prover as a reference on all three meters and in addition will have the ability to perform master metering to check the behavior of the turbine and the second ultrasonic meter using one of the ultrasonic's as a master. If we can perform parallel batching and master metering, this will provide us measurement from two different loops (mechanical and electronic) to compare their performances.

3.1 Testing the Design at a Calibration Agency

It was agreed with the manufacturer from the outset that this type of arrangement has to be tested at a calibration agency to gain some confidence in the results prior to installing on site. The test was setup at SPSE in France. The turbine meter from Saudi Aramco was sent to SPSE along with the two ultrasonic meters. Due to heavy usage of the calibration facility, a window was booked for testing the design. It was agreed that such testing would provide a good reference for the design to work in the normal day-to-day operation.

Several tests were performed on liquids with similar viscosity ranges to those to be measured in the field. The test performed at SPSE showed good results and provided some confidence the setup would at least provide a reasonable basis for testing the design.

3.2 The Field Setup View

The test setup is believed to be unique both in terms of size of the equipment being used and the types of tests being performed in a synchronized manner. Fig. 6 shows an overview of the field setup. The new loop is shown here



Fig. 6 U-Shape arrangement with three meters in series

It can be seen in Fig. 6, the mechanical engineering necessary to design and install the loop. The U-Shape comprises of three * 20 inch meters (one turbine and two ultrasonic). The existing meter stream was modified to fit this design into the same flanges that previously held the turbine meter stream. The structure connects at both ends of the previous meter stream, only now with three meters in series. The 42" prover is the second U-Shale below.

The phase 2 test loop design meets API requirements for each meter installed. Any liquid flowing in the line will flow through all 3 meters. There is no other path for the liquid to go. As can be seen considerable design modifications were required to not only setup the test but to install the new loop. This is on an offshore platform.

This unique design will provide a good basis for testing this technology

3.3 The Measurement System Setup

The mechanical loop designed for this setup allows liquid to flow though all the meters. This will ensure each meter will see the same liquid to be measured. However, to perform the various measurement functions, this has to be designed into the metering measurement/control system.

It was decided from the outset that the official delivery to ships was to be performed by the Saudi Aramco metering control system. In other words, the turbine/prover combination measurement functions will be performed by the Saudi Aramco metering control system. The start and end batching commands, proving, etc. are all to be performed by the Saudi Aramco metering control system. This will ensure there is very little impact on the normal daily operations. A separate test measurement system is to be setup that will use the various signals from the Saudi Aramco system to perform the required functions as a shadow – namely batching, proving, master metering, etc. and all to be performed automatically. The test measurement system will work independently while the loop is being used in any custody transfer. The field signals are shared between the two systems.

A separate panel was designed comprised of flow computers, manufacturer flow processors, and metering supervisory to integrate the complete test measurement requirements of batching, proving, master metering independent of the official delivery system.

Fig. 7 shows the architecture of the test measurement system. The system uses flow computers for performing the various measurement tasks. Each meter has its own dedicated flow computer.

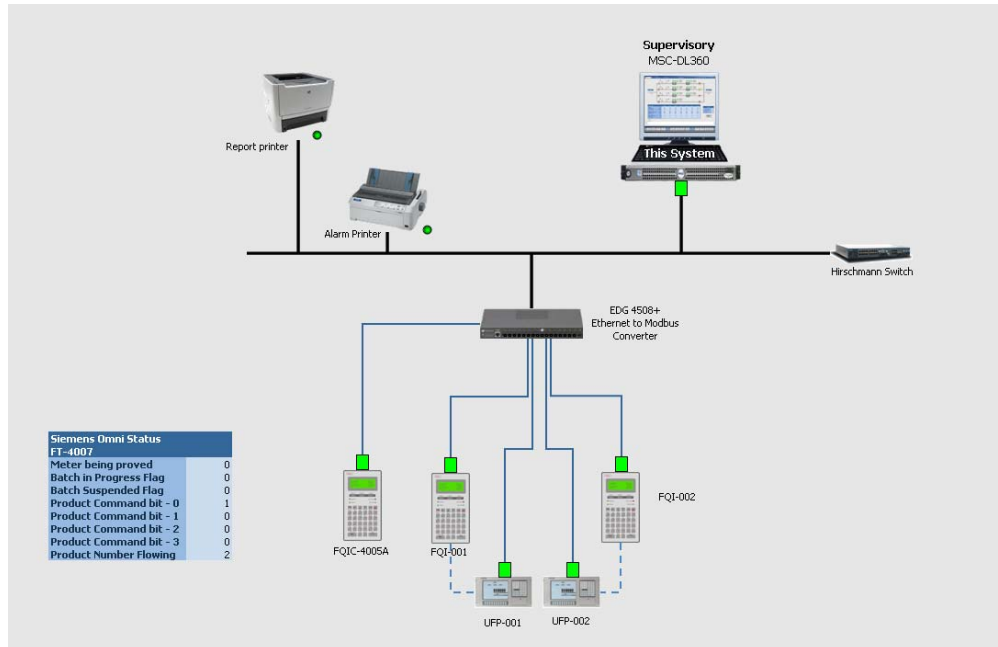


Fig. 7 Measurement system setup

The control of the loop is under the Saudi Aramco metering control system. The setup initiates data collection as soon as the loop is open for loading. Any liquid flow is captured by the three flow computers. Certain data from the Saudi Aramco system is copied by the test measurement system like batch number, etc. as shown in Fig. 8

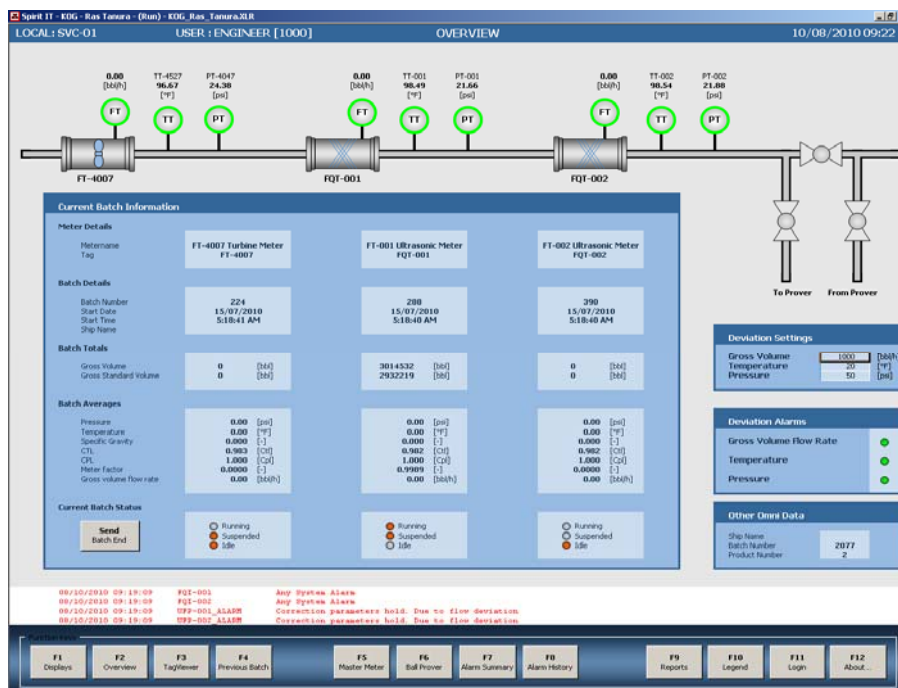


Fig. 8 Batch data for the 3 meters

Proving is performed on all three meters once in a batch. However, the system is setup to perform master metering every two hours in a batch. This will enable data to be collected showing the performance of the meters during the complete batch.

The system enables us to prove a meter using the conventional method and repeat the test using master metering. This will enable comparison of each meter performance as stated by the prover and the master metering method.

Initially, the master metering arrangements were such that the turbine would act as a master. However, this was changed with one of the ultrasonic meters dedicated as a master checking the turbine and the second ultrasonic meter. The prover will provide the performance of all three meters.

3.4 Types of Tests to be Performed

The primary goal for testing this technology is to establish whether it can perform to the same level or better than the accepted mechanical technology that has been going strong for the last 50 plus years. Despite considerable testing to date on this technology, a clear path has not been adopted.

The design adopted in this paper as stated above allows a number of tests to be performed as a direct comparison which to the best of the authors' knowledge has not been performed elsewhere in the world. This setup provides various scenarios to be tested between the conventional turbine/prover and the master metering arrangement within the same batch with full assurance that all the measurement devices are seeing the same liquid. This will provide a direct comparison of what is being reported in terms of volume or meter performance, etc. by the currently accepted loop (mechanical) and the master metering loop (electronic loop). We will be able to see what each is reporting with the hope they will be the same or if not, it will provide a basis for investigating their differences.

Typically the tests will be:

1. Proving using the ball prover on the three meters
2. Batching with volume comparison of turbine/prover vs. USMs (ISV, GSV using historical curve, GSV using current proof).
3. Master metering with USM as master on turbine and second USM.
4. Prover on three meters vs. master metering
5. Volume comparison from both loops

This will provide ample data for the various comparison tests on the performance of the presently acceptable turbine/prover (mechanical loop) and the master metering using ultrasonic meters (electronic loop).

4 THE TEST SYSTEM COMMISSIONING

The test system was commissioned in February 2010. Considerable effort was required from Saudi Aramco personnel to design and install the measurement loop as shown in Fig. 6. Dedicated support was provided from the manufacturer during this phase of the work and in the installation and commissioning of the test system. As expected, there were some logistical issues, system issues, etc. that needed to be resolved.

The test system was finally commissioned successfully. During commissioning, some additional modifications to improve the test system design were proposed. Some of these were addressed during commissioning and others were developed and installed at a later date.

There have been some logistical issues that have prevented us from setting up the complete system for the data collection phase. These are being addressed. It is envisioned additional

data to what is being presented will be available prior to the submittal of the presentation material.

5 INITIAL RESULTS

The sections below provide preliminary results from the test setup at Saudi Aramco.

5.1 Ball Prover Results

At this stage of the testing, only a limited data set has been captured. Fig. 9 gives the proving results of the three meters under test for Arabian Light crude oil. The data shows the turbine meter in need of larger correction as stated by the prover. This is in line with the known performance of this meter for this type of crude oil.

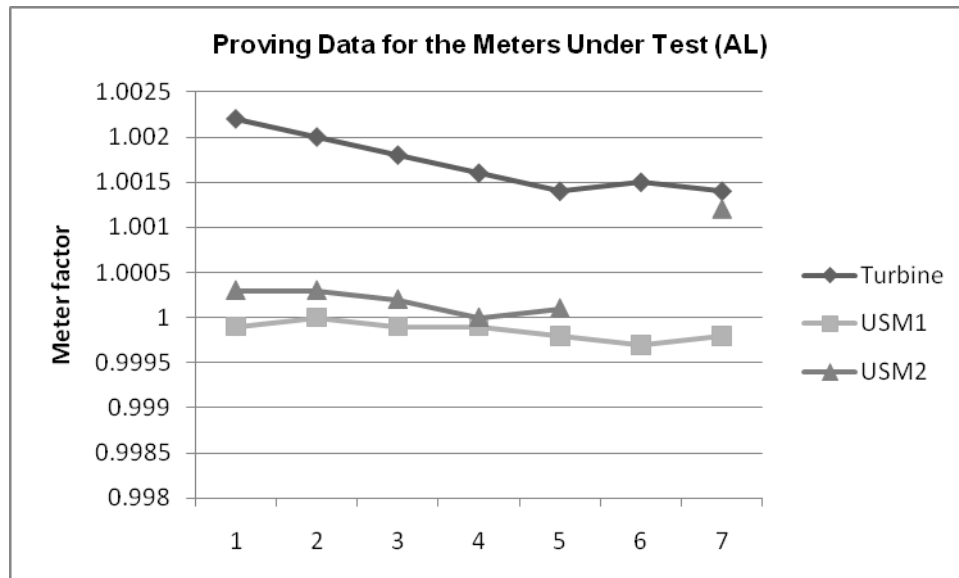


Fig. 9 Proving results for the three meters under test

Fig. 9 also shows the prover stating that the two ultrasonic meters are very close to reporting the actual flow without needing much adjustment. This would imply the reported standard volume of the two ultrasonic meters without any prover influence will be close to the delivered volume while the turbine will have to be adjusted using the meter factor accordingly. It will be shown in a later section how these are reflected in the final volume delivered.

5.2 Master Metering Results

Fig. 10 shows the master metering of the turbine meter as a master over the ultrasonic meter. Our expectations are to see how this links with Fig. 9 above since it is for the same crude type. We would expect to see the same result for Arabian Light from this testing as was seen from Fig. 9. Unfortunately, the data collected for this test was at a much higher flow rate than in Fig. 9 and hence a direct comparison cannot be made. However, it does show about a 0.5% change in the slope which is a concern and needs to be investigated.

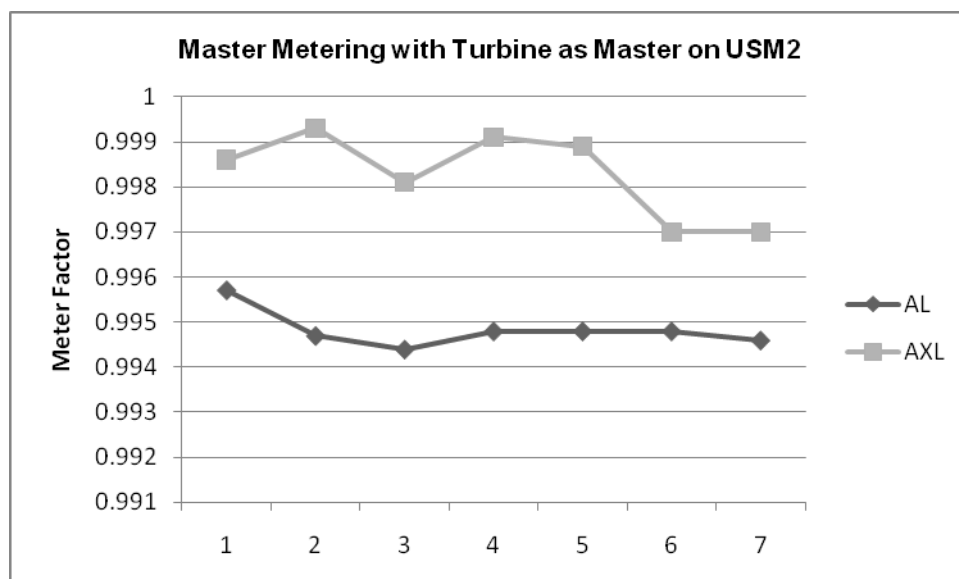


Fig. 10 Master metering turbine on USM

Table 1 shows the meter factor reported by the master meter method with USM 2 as the master on the turbine meter. For the same turbine meter using a prover for the first flow rate, the meter factor reported by the prover is 1.0018. This amounts to a difference being reported by the two loops of 0.05%. This is an encouraging result for the test setup.

Table 1 – Master metering USM 2 (600001) as master on turbine for AL

Flow Rate	11,122	11,262
Meter Factor	1.0023	1.0019

The master metering of one ultrasonic on another is presented in Fig. 11. It can be seen from the scatter the variation in meter factor. The change for Arabian Light crude is around 0.05% and for Arabian Extra Light is about 0.129%.

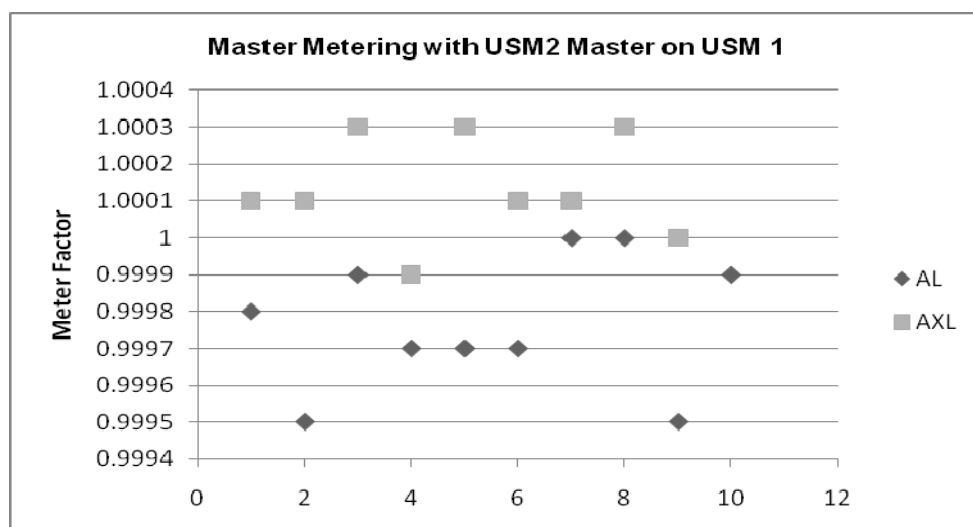


Fig. 11 Master metering with USM on USM

5.3 Batching Results

Table 2 and Table 3 represent a comparison of the gross standard volume being reported by the turbine/prover combination being compared with each USM indicated standard volume (no prover adjustment), the USM gross standard volume with prover meter factor applied and in one case USM gross standard volume with master metering meter factor applied.

Table 2 – Turbine/Prover GSV compared to USM 2 (600001) for AXL

Batch Volume Size	159,640	131,998
Indicated Standard Vol.	- 0.046%	-0.03%
Gross Standard Volume – Proving Meter Factor	- 0.136%	-0.13%
Gross Standard Volume – Master Metering Meter Factor		

Table 3 – Turbine/Prover GSV compared to USM 1 (25821210) for AXL

Batch Volume Size	159,640	131,998
Indicated Standard Vol.	+ 0.05%	+0.03%
Gross Standard Volume – Proving Meter Factor	-0.025%	-0.13%
Gross Standard Volume – Master Metering Meter Factor	-0.005%	

In reference to Tables 2 and 3, it can be seen for the case of the first batch, the uncorrected volumes for both meters are in close agreement; however, when they are corrected by the meter factor from the prover, the final volumes differ considerably. However, the same is not true when the master metering meter factor is applied to the final volume. In this instance, the final volume is much closer to the delivered ship value. Clearly something is not quite right and will need to be investigated. However, in the case of the second batch, both meters are in very close agreement to each other, but the result of applying the prover meter factor degrades both meters results equally.

Table 4 and 5 shows both meters reported volume to be different by an unacceptable amount from the turbine/prover reference volume for the Arabian Light crude. The master metering improves the result in the case of the second batch. This will need to be investigated.

Table 4 – Turbine/Prover GSV compared to USM 2 (600001) for AL

Batch Volume Size	268,516	81,345
Indicated Standard Vol.	- 0.289%	-0.268%
Gross Standard Volume – Proving Meter Factor	- 0.3%	-0.268%
Gross Standard Volume – Master Metering Meter Factor		-0.089%

Table 5 – Turbine/Prover GSV compared to USM 1 (25821210) for AL

Batch Volume Size	268,516	81,345
Indicated Standard Vol.	-0.265%	-0.237%
Gross Standard Volume – Proving Meter Factor	-0.24%	-0.21%
Gross Standard Volume – Master Metering Meter Factor		-0.058%

Tables 6 and 7 provides comparison of batching data between the two ultrasonic meters for various size batches. It can be seen that there are consistently coming close to each other for the two types of crude being measured.

Table 6 – Comparing ISV of USM 2 (600001) to USM 1 (25821210) for AL

USM 2 (600001) Batch Size	186,625	267,739	199,177	195,845
USM 1 (25821210) Batch Size	186,722	267,804	199,207	195,889
Deviation %	-0.052%	-0.024%	-0.015%	-0.022%

Table 7 – Comparing ISV of USM 2 (600001) to USM 1 (25821210) for AXL

USM 2 (600001) Batch Size	159,567	131,958	59,033	233,992
USM 1 (25821210) Batch Size	159,648	132,038	59,049	234,050
Deviation	-0.05%	-0.06%	-0.027%	-0.025%

6 SUMMARY

The results reported in this paper were obtained from the test measurement system with the loop being used for official deliveries to ships. The turbine meter and the prover are used for billing purposes, while data from the ultrasonic meter for the same delivery is used for the comparison tests. As stated, a parallel test measurement system performs all the required measurement functions and collects and archives the data. This test measurement system has no control over the measurement loop and performs all the necessary functions as a shadow system to the one being used in the official delivery. It performs these functions automatically without the need of any manual intervention. The operation staff use the turbine meter as they have done in the past. The difference now is that we have three meters in the same loop that are reporting to the test measurement system.

Some positive results were obtained from phase 1 testing of this technology as is reported in Section 2 of this paper. We have shown the ultrasonic meter while not impacted in the same way as the turbine for the different liquids to be measured, is never the less not totally linear for the types of liquids for which it was tested. This implies the need to calibrate the meter on-site for the liquids for which it will be used for measurement. This was despite being calibrated for the range of liquid viscosities at a calibration agency.

In Section 2.2, it was shown that the ultrasonic meter cannot be used by itself without a prover. However, there are some encouraging results when the meter is used with only a calibration curve and not having the prover correct its performance online as is the case with the turbine meter. The testing for this aspect will be closely observed. From the results, it is quite feasible one of the options will be acceptable; either reduce the prover usage while being online or remove it to a central location and only use the historical curve. In either case, it will provide significant benefit over the current scenario of having to use the prover every batch.

The proving repeatability of these ultrasonic meters has been highlighted in many publications including API Chapter 5.8 [5]. The data provided in [5] does not cover the meter/prover size being used in this test; however, [5] states that the number of runs required are far greater than what has been achieved in this test as shown in Fig. 5. This is a subject of further investigation.

The test measurement setup is unique both in terms of the size of meter being tested and types of tests being performed. It is hoped the results obtained will help to decide the use of this technology in the best configuration – without the direct need of mechanical prover. However, it is early to make any predictions.

The test measurement system has been commissioned and while some results have been reported, considerable more data needs to be collected on the various types of tests being proposed in this paper.

From the limited data available, it can be seen the prover is reporting the turbine meter in need of large correction, more so than the ultrasonic meters. This is in line with the results found in phase 1 as shown in Fig. 3.

The master metering of the turbine meter using one of the USM also shows close reporting of the meter factors between the mechanical loop and the electronic loop. However, due to only a couple of points being available, it is difficult to make any judgment. This will be followed closely as it is a critical test.

The master metering of ultrasonic meters show how close they are reporting their performance. This is to be expected and over the testing period will help in deciding if the master metering is adopted, and how to establish controlling limits when checking master/duty meters.

Tables 2 -7 provide various batching data. It is clear from these the ultrasonic meters are reporting volume close to each other, but not necessarily close to the reference loop which is the turbine/prover. One point that has been observed is while the prover is stating the ultrasonic meters are over stating their volume, the final batch value does not reflect this. This is one of the reasons when a prover correction is applied the final result is degraded rather than improved. This is another point that needs to be investigated.

7 ACKNOWLEDGMENTS

The author would like to express his sincere thanks to:

Saudi Aramco management, Process & Control System Department management and to the field partner management – Terminal Operation and Maintenance Departments for providing the necessary resources for testing this technology and to.

Custody Measurement Unit and the Petroleum Loss Control Unit for their tireless support.

KROHNE Oil & Gas for all their support.

8 REFERENCES

- [1] Boer, A., KROHNE Altometer, "Ultrasonic Multibeam Flow Measurement for Liquids – A new technology for custody transfer applications".
- [2] Dahlstrom, M. J., Norsk Hydro ASA, "Effortless Oil Ultrasonic Fiscal Meter Operation: KROHNE Altosonic-V, with Master meter approach", 18th North Sea Flow Measurement Workshop, 2000.
- [3] Moon, C. B., BP Amoco Exploration – Forties Pipeline System, "Field Trial of the KROHNE 5-path meter on Forties Blend at Dalmeny Export Terminal".
- [4] Boer, A., Leenhoven, T., Danen, H, KROHNE Altometer, "Multbeam Ultrasonic Flow meter for custody transfer: Experiences and Calibration", May 2001.
- [5] American Petroleum Institute, Manual of Petroleum Measurement Standards, Chapter 5.8.

Paper 6.3

Fiscal Oil Ultrasonic Meters: Introducing the Calibration Performance Monitoring (CPM)

**Denis Laurent
Metering & Technology SAS**

Fiscal Oil Ultrasonic Meters: Introducing the Calibration Performance Monitoring (CPM)

Denis Laurent, Metering & Technology SAS

1 ABSTRACT

Off-site calibration of USMs is now considered in more and more applications and projects:

- The cost of a displacement prover is not acceptable for the project,
- The big size of the meter will lead to an unacceptable volume for the prover,
- Ultrasonic Master Meter is preferred, due to their unique features in terms of CAPEX / OPEX savings and to their wide operational range.

So securing the transition from calibration laboratory to field is of primary concern.

Thanks to their large number of ultrasonic beams, a new generation of meters give a rich and reliable access to quantitative, traceable and accurate information on the velocity profile inside the metering section.

From these data, a new validation method is built: the Calibration Performance Monitoring.

This new method is fully in phase with the API recommendation, which encourages users to monitor internal diagnostic parameters and to compare them to the lab determined ones.

It is valuable at every stage of the meter's life:

- at calibration time, to validate the installation
- at commissioning time, to validate the error of the meter
- as a powerful tool for periodic verification, to decide if a recalibration is necessary or not,
- as a real-time alarm tool, to protect the metering system against an unexpected change in conditions between proves.

2 INTRODUCTION

Ultrasonic meters are in phase with the quick evolution of general instrumentation.

- Advances in material science: namely piezo-composite ceramics,
- Advances in mainstream electronics: power doubles every 18 months,
- Specific advances in medical ultrasonic imaging: components and algorithms.

Clearly, USMs have not exhausted their potential. Major trend for the future are:

- low power electronics,
- ultra-fast scanning rates,
- more ultrasonic beams.



1999 2008

As we will see, these advances have serious operational consequences.

3 FLOW TOMOGRAPHY: The Holy Graal?

It is well known today: no USM can cover the full industrial range of flow profiles and Reynolds Numbers from naphthas to heavy oils by simply summing the velocity measurements over the acoustic paths ... at least not within a 0.15% accuracy.

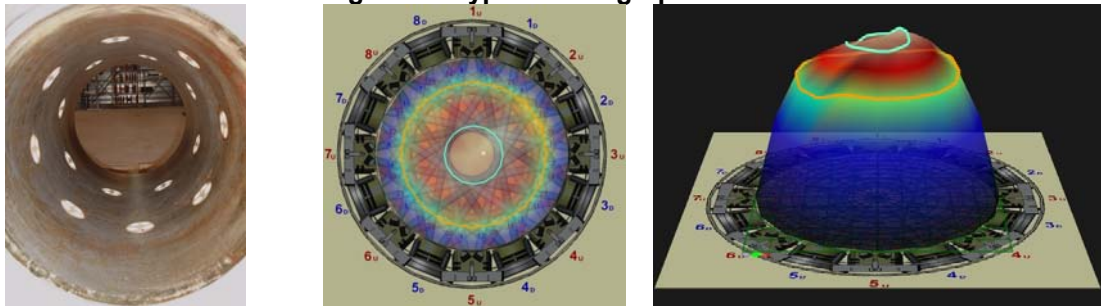
So every meter needs some amount of "flow calibration".

With much more beams available, it could look reasonable to get rid of this costly "flow calibration" by tomographic techniques.

The basic idea of flow tomography is:

- to divide the metering section in M small cells
- to compute the velocity (V_i) in each cell from the velocities over the N paths (U_j)
- finally to sum all the cell velocities so as to get the flowrate

Figure 1 - Typical tomographic views



This is not the place to expose the theory of tomography, but an important result is to keep in mind : the solution of the tomographic problem (i.e. find the V_i from the U_j) is univocal if, and only if, $M = N$, i.e. number of cells = number of beams.

For example, a 32 beams will only solve exactly 32 flow cells, which is rather low resolution.

It is of course possible to get images with better resolution, but it does require some non-exact numerical manipulations (modelling, extrapolations, ...)

Let's develop.

$$V_i = [A] U_j \quad \begin{matrix} V_1 = a_{11} U_1 + \dots + a_{1n} U_n \\ \vdots \\ V_n = a_{n1} U_1 + \dots + a_{nn} U_n \end{matrix} \quad \begin{matrix} \text{where :} \\ A \text{ is a } [n \times n] \text{ matrix.} \\ a_{ij} \text{ are constant coeffs.} \end{matrix}$$

$$\begin{aligned} \text{Flowrate is : } Q &= (\pi D^2 / 4) (V_1 + \dots + V_n) \\ Q &= (\pi D^2 / 4) [(a_{11} + \dots + a_{n1}) U_1 + \dots (a_{1n} + \dots + a_{nn}) U_n] \end{aligned}$$

$$\text{so, finally : } Q = (\pi D^2 / 4) (k_1 U_1 + \dots k_n U_n) \dots$$

... which is not more than the weighted sum of the ultrasonic velocities !

So, as far as the concern is to compute flowrate, a "honest" (assumption-free) tomographic method is not more that the weighted sum of the velocities ...
... unless we make some "assumptions" on the shape of the flow profile to be metered ...,
... but who would accept oil transactions based on "assumptions" ?

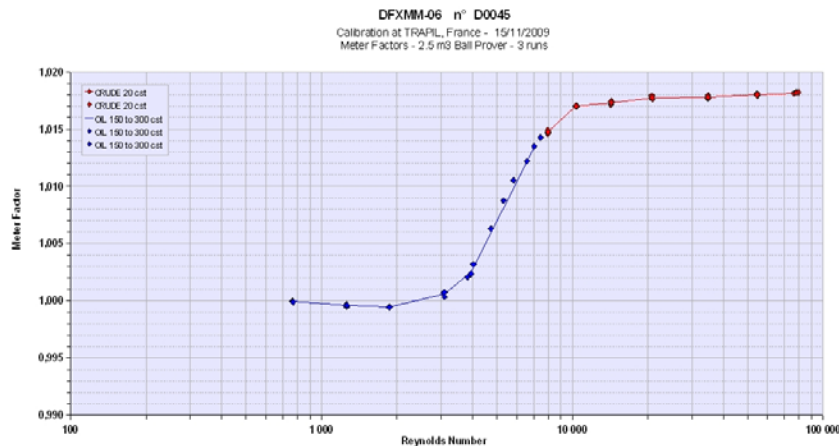
More seriously, tomography is probably the future of ultrasonic metering, but much further research is needed to make it acceptable at fiscal quality level.

We, at M&T, already have a foot in it and strongly encourage R&D on this topic.

4 LABORATORY CALIBRATION and its LIMITS

4.1 Flow Calibration Basics

Figure 2 - Typical error curve - uncalibrated 6"meter, 20 to 300 cst



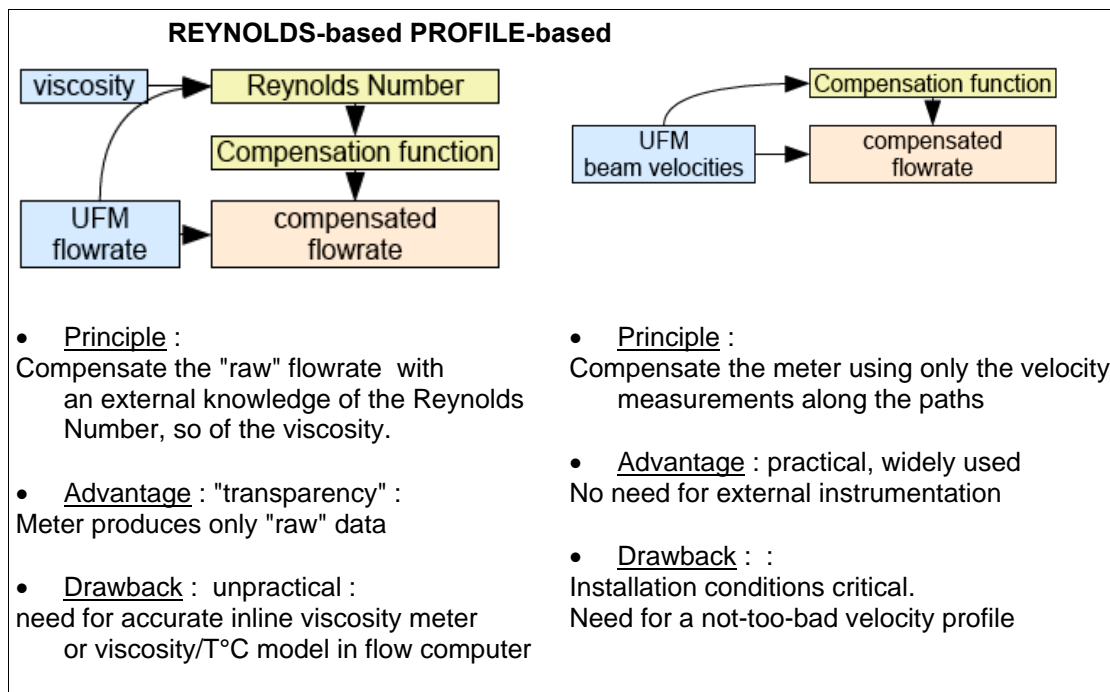
Here is a typical "raw" error curve from an uncalibrated 6" USM over a wide viscosity range. ("raw" means : just the weighted sum of the path velocities).

Results could be slightly different with different path positions or different weighting coefficients, but overall shapes as above are well known from experience.

- linearity is fiscally acceptable for Reynolds Numbers (RN) above 10 000 (i.e. less than 20 cst in a 6" meter) and below 2 000 (more than 300 cst in a 6" meter)
- Meter Factor is shifted +/- 1% within the turbulent-to-laminar transition zone because of the drastic change in velocity profile. (for our 6" meter, this means from 20 to 300 cst, i.e. very common operating conditions).

So some kind of compensation is mandatory. Here are the classical methods :

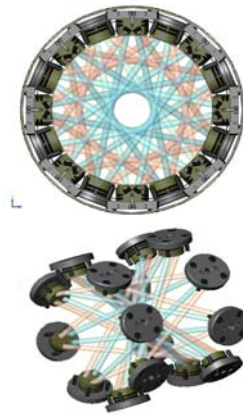
Figure 3 - Flow calibration techniques



4.2 Profile-based Flow Calibration: a practical example

The meter is made of:

- 16 **BLUE** paths located roughly at **0.25 R**,
- 16 **RED** paths at **0.75 R**.



Flowrate is : $Q_{m3/h} = (3600 \cdot \pi \cdot D^2 / 4) \cdot (1/32) \cdot \text{Sum}(V_i) \cdot \text{Calibration Function}$

The meter is said "uncalibrated" when the Calibration Function is set to 1.000 .

The ratio " **blue** / **red** " velocities is used as an input for the calibration function.

Let's name it: **PROFILE NUMBER (PN)**.

(Also know as 'shape factor', 'flatness ratio', ... but the concept is the same)

It is a non-linear function (f) of the Reynolds Number (RN) only.

It is computed and logged in real-time by the meter.

High Reynolds N° :

"flat" velocity profile

blue and **red** velocities give close results

Low Reynolds N°

"parabolic" velocity profile

blue over-count and **red** under-count.

In a similar way, the **RAW METER FACTOR (RMF)** of the uncalibrated meter is another non-linear function (g) of the Reynolds Number (RN) only.

From the (f) and (g) functions, we build a third function (h), which describes the **RAW METER FACTOR (RMF)** versus the **PROFILE NUMBER (PN)** .

This function (h) is independent on the Reynolds Number (RN).

It is the calibration function to be entered in the memory of the meter.

$$\text{RMF} = f(\text{RN}) + \text{PN} = g(\text{RN}) \Rightarrow \text{RMF} = h(\text{PN})$$

Step #1 :

Proving to establish the
RAW METER FACTORS (RMF)
v/s Reynolds Numbers (RN)

Linearity is +/- 1% from 20 to 300 cst.



"raw curve" $RMF = f(RN)$

Step #2 :

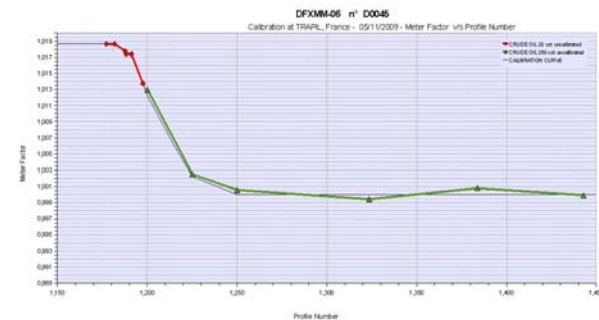
simultaneously record the
PROFILE NUMBERS (PN).
(**BLUE/RED** ratios)
v/s Reynolds Numbers (RN)



"profile curve" $PN = g(RN)$

Step #3 :

Combining (f) and (g) so as to get
a third function (h) $RMF = h(PN)$,
which is now independent on RN.
It is the **CALIBRATION FUNCTION**



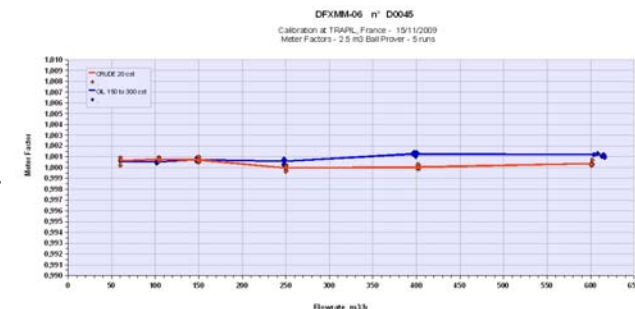
"calibration function"

$$RMF = f(RN) + PN = g(RN) \Rightarrow RMF = h(PN)$$

Step #4 :

Enter this curve (h) in the meter
and prove for validation.

Linearity is +/- 0.1% from 20 to 300 cst.



4.3 Flow Laboratory Calibration: the limits

It is not exactly true that both the "raw curve" and the "profile curve" depend only on the Reynolds Number (RN).

Actually, they depend both on the RN and on the installation conditions.

And of course, installation conditions at final location will not match the lab ones, each difference being a potential source of systemic error, with its own sensitivity coefficient.

Figure 4 - Possible differences from lab to field

" FAR UPSTREAM " conditions	<ul style="list-style-type: none"> - inlet geometry (elbow, tee, manifold) - valve - straight length - reducer angle - number and location of flanges - piping schedule & rugosity - intrinsic turbulence level ...
" NEAR UPSTREAM " conditions (between FC and meter)	<ul style="list-style-type: none"> - straight length - schedule & rugosity - orientation of Flow Conditioner - concentricity - gaskets ...

Even if most sensitivity coefficient are individually small, their sum may be significant: ten independent errors as low as 0.1% will combine to give a 0.32% global error.

More problematic, undetected accidental errors are possible : protruding gasket, bad piping concentricity, misalignment of the flow conditioner,...

These sources of error are only evaluated in very rare "type approval" tests.

They are quasi-impossible to evaluate individually on a case-by-case basis :

- the final detailed geometry of the metering skid is often unknown at lab calibration time,
- we, manufacturers, have to confess that we sometimes accept situations where the meter is not calibrated using its final upstream piping.

As a consequence, it is a common practise of our industry not to document the effects of installation as seriously as necessary, and to consider that the overall effect is a small and constant shift of the Meter Factor from lab to field, which is detected and corrected at field proving time.

This policy is acceptable in a lot of situations, mainly when Reynolds N°s are greater than 10 000 or smaller than 2000.

But what if ...?

Figure 5 - Some situations at risk when ignoring installation effects	
1	USM to be used as a MASTER METER
2	Reynolds N°s between 2 000 and 10 000 (for a 6" : 20 to 300 cst, for a 16" : 50 to 800 cst)
3	Accuracy / reliability of the proving device (displacement, master, tank) is less than the accuracy of the calibration lab
4	No Field Prover

These metering situations are obviously from the real world,

They are usual, as off-site calibration is now considered in more and more projects :

- The cost of a displacement prover is not acceptable for the project,
- The big size of the meter will lead to an unacceptable volume for the prover,

- Ultrasonic master meter is preferred, due to their unique features in terms of CAPEX / OPEX savings due to their wide operational range.

5 Taking ADVANTAGE OF MORE BEAMS

5.1 Axial Symmetry

The first obvious advantage of more beams is the high degree of symmetry, which minimizes the adverse effects of severe distortions in the flow profile.

Figure 6a - Comparison of 4 and 32-beams meters response to severe asymmetry (CFD study)

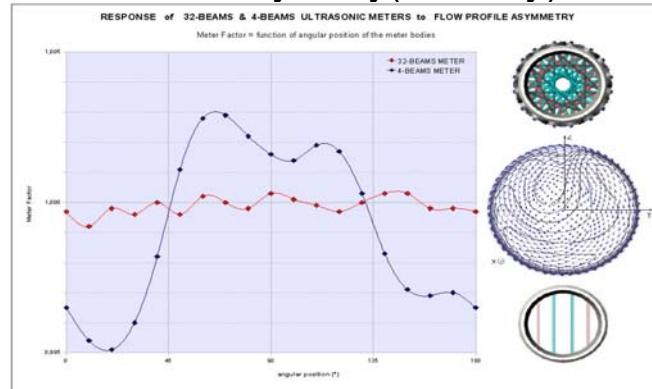
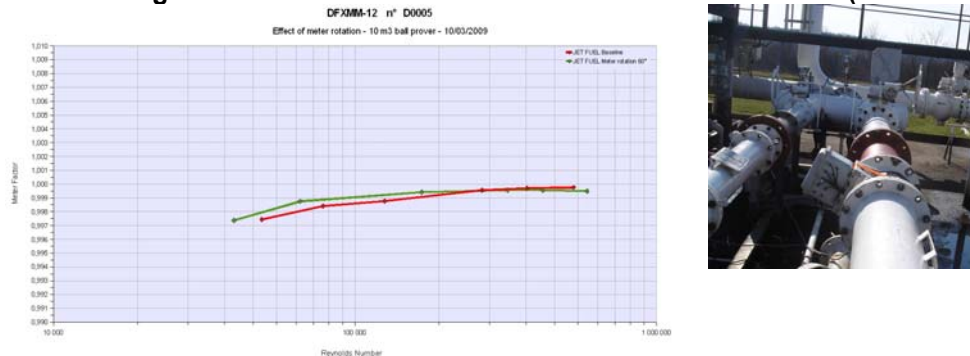


Figure 6b - Effect of meter rotation on a 32-beams meter (field test)



This is a serious advantage where sufficient straight piping is not available, or where flow conditioner is to be avoided - namely offshore -. The advantage is much less evident with normally sized metering runs, where flow profile is (supposed to be) axi-symmetrical.

4.2 Velocity Patterns

The second obvious advantage of more beams is to enable a rich, real-time information on the structure of velocities in the metering section.

Namely, it is possible to record the Velocity Patterns found at calibration time - for each calibration flowrate and viscosity - and to compare them later to what is found on the field.

**Figure 7a - Typical Velocity Pattern
at calibration time**

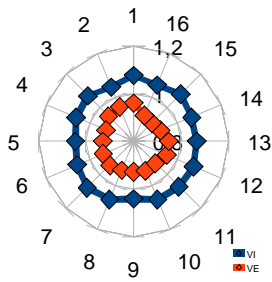
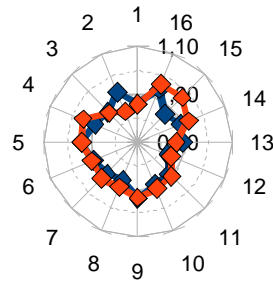


**Figure 7b - Typical Pattern difference from
laboratory to field.**



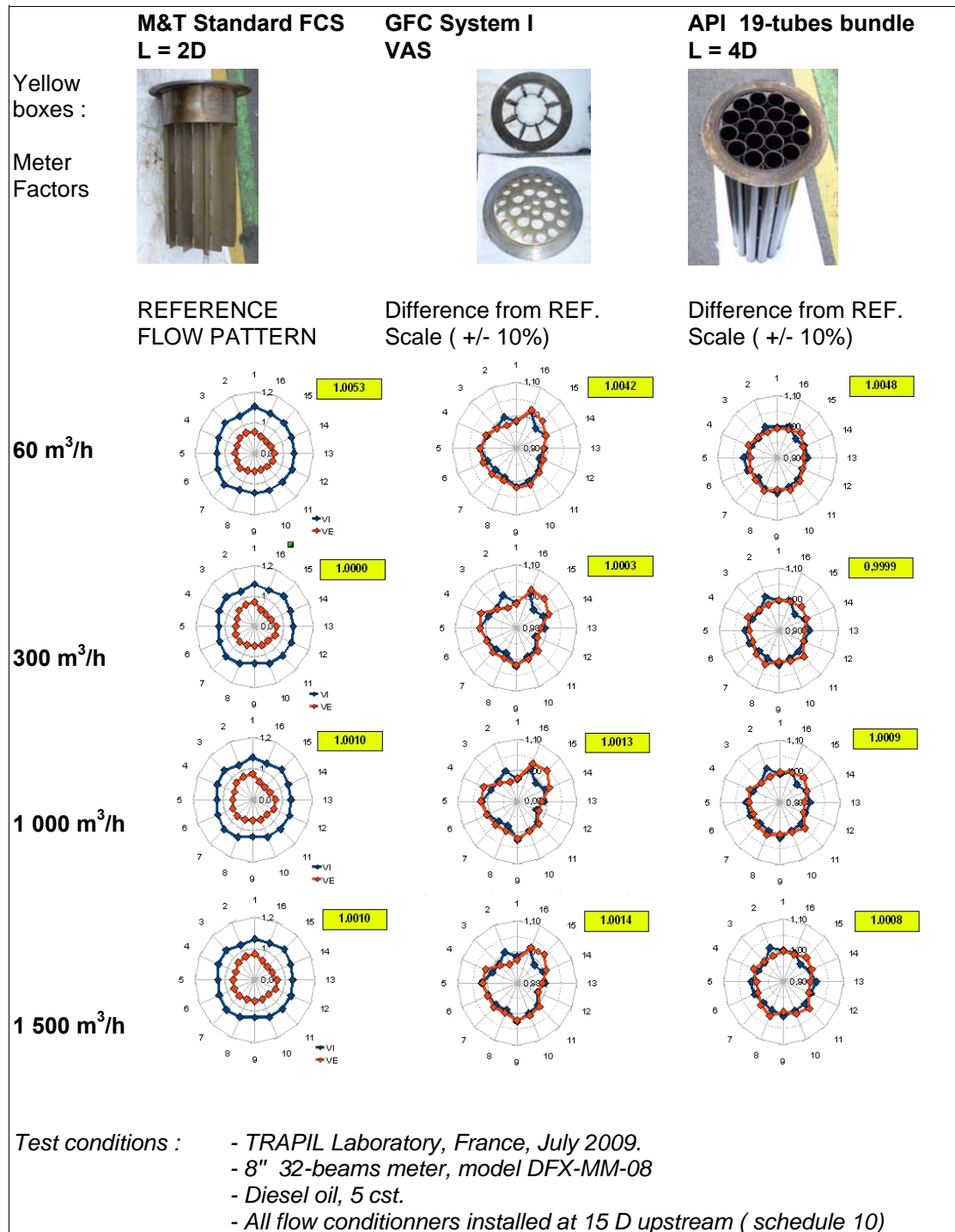
This approach is in phase with the API recommendation concerning liquid USM :

API MPMS ch5.8 "Ultrasonic Meters" &14 : Diagnostics

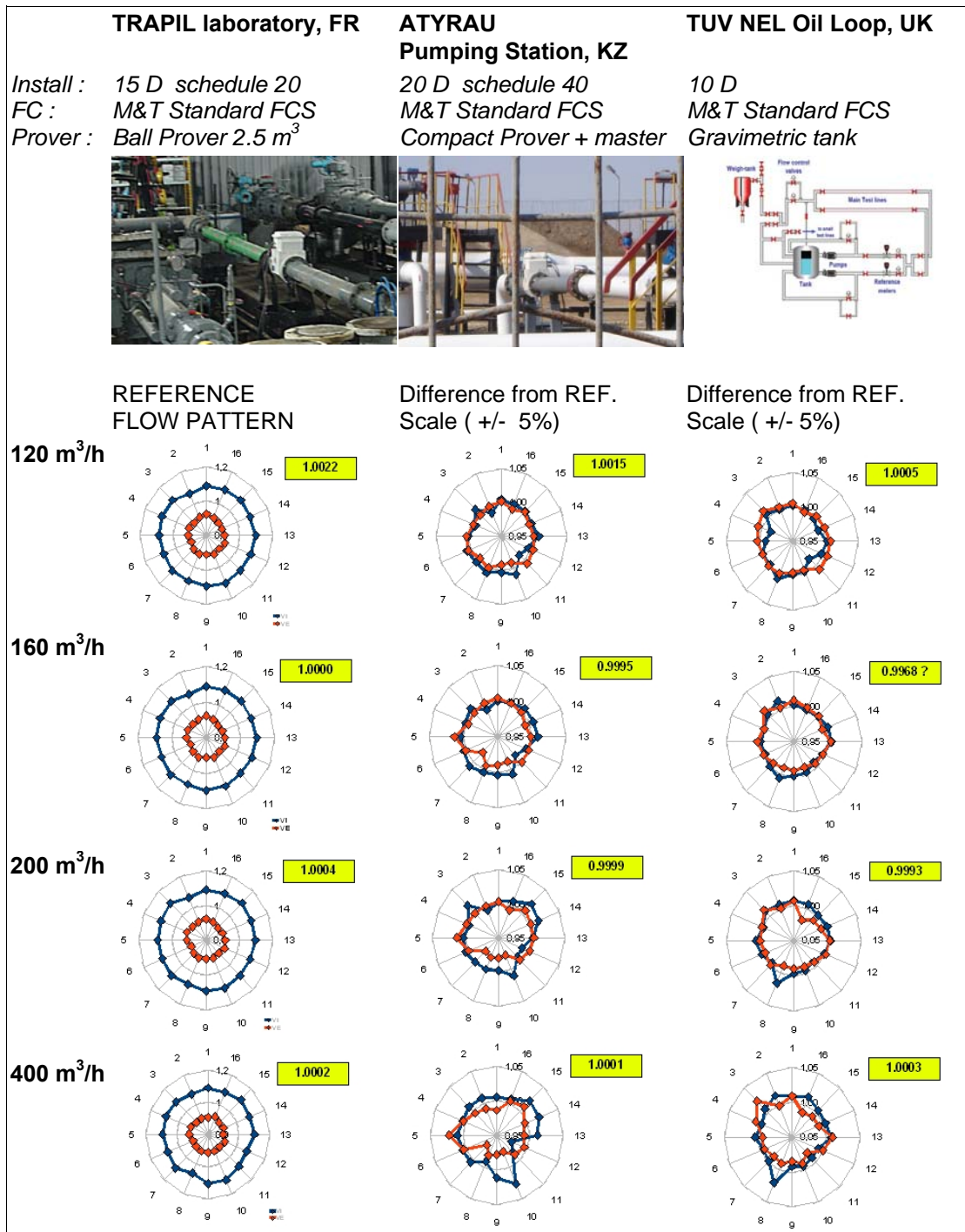
" Certain parameters can be monitored based on the specific application. ... Comparing lab determined diagnostic parameters to the same parameters when installed in the field may help identify field installation effects or other parameter changes. It is also recommended to compare these parameters periodically during meter operations."

Let's develop further.

4.3 Case study #1 : 8" meter with different Flow Conditioners.



5.4 Case study # 2 : 6" meter on different sites and different upstream conditions



The striking result of these two case studies is that, despite the significant differences in installation conditions, the Meter Factors found for each flowrate are very similar - within 0.1% -, as soon as the Velocity Patterns are "reasonably close".

A rule of thumb could be that Meter Factors do not differ by more than 0.1% when Velocity Patterns do not differ by more than 2%.

In other words :

SAME INPUTS => SAME OUTPUT

6 CALIBRATION PERFORMANCE MONITORING (CPM)

6.1 Principle of CPM

The basic principle "Same inputs, same output" could look rather trivial.

But, as far as the "input" information is rich - which is the case for a 32-beams meter -, it is possible to take serious operational advantages of it.

Just an example:

"Same inputs => same output" means : No change in pattern => No change in Meter Factor.

In other words : *no need to prove again or no need to re-calibrate !*

Clearly a way to cut the cost with a better schedule of periodic verifications / recalibrations in the context of a Condition Based Maintenance (CBM) program.
(imagine a 24", 3000 lbs meter located 100 NM offshore ...)

Based on the results above, M&T developed a new method and implemented it as follow :

Figure 8 - The CPM method

CALIBRATION	<ul style="list-style-type: none"> - Velocity patterns are logged, for each calibration flowrate and viscosity. <i>Example : 6 calibration flowrates * 3 oils = 18 patterns</i> - Validated patterns are stored in the meter memory as references.
OPERATIONS	<ul style="list-style-type: none"> - Current pattern is compared to reference at closest flowrate & viscosity. - Meter software checks for acceptance and manage alarm accordingly. - The comparison/validation process is automatically performed in real-time.

Using procedures based on Calibration Performance Monitoring (CPM) is valuable at all steps of the meter life :

Figure 9 - Calibration Performance Monitoring (CPM) values

CALIBRATION	validate meter installation qualify lab flow profile validate efficiency of flow conditioner	<i>- detect a protruding gasket, a bad concentricity, ...</i>
COMMISSIONING	validate skid piping & meter installation	<i>- same</i>
PERIODIC CHECK	schedule not only by law, but when needed, under CBM program	<i>- No change in pattern => no change in Meter Factor</i>
ANY TIME	reliable "out-of-fiscal-performance" real-time alarm	<i>- foreign object in the FC - abnormal dirt or wax deposit - loss of beams due to gas - run valve not 100% open</i>

It is of special value in situations at risk as described in § 3.3 and Figure 5.

6.2 CPM : practical implementation

The main concerns when Implementing a practical, real-time CPM method are :

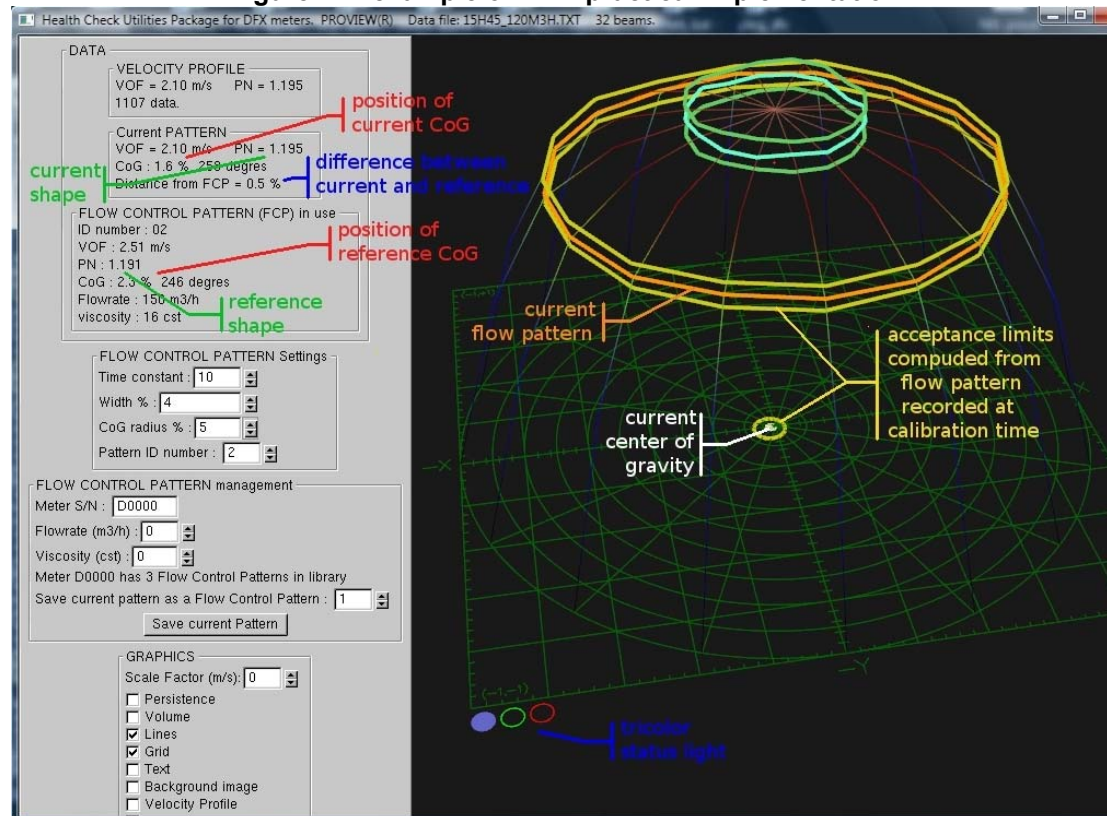
- provide quantitative, traceable and auditable data about the Velocity Pattern, so as to make them available to any authority involved,
- provide a reliable GO-NOGO (fiscal-nonfiscal) real-time quality indicator, so as to make it available through the supervision to any operator without special metering skills.

6.2.1 CPM data

Figure 10 - CPM real-time quantitative data

Reference 32 Velocities from the calibration laboratory	controls the <u>quality of lab conditions</u>
Current 32 Velocities	indicates the " <u>shape</u> " of the velocity profile
Position of the CENTER of GRAVITY angle from vertical + position in % of R	controls the <u>upstream conditions</u> & the <u>concentricity of piping</u>
PROFILE NUMBER ratio BLUE beams / RED beams	controls the " <u>flatness</u> " of the velocity profile
SWIRL INDEX	controls the <u>efficiency of flow conditioner</u>
" DISTANCE " in % between current and reference patterns	controls the <u>similarity to lab conditions</u>

Figure 11 - example of CPM practical implementation



The information is available through the numerical link of the meter.

6.2.2 CPM real-time indicator : Blue, Green, Red

Acceptance limits are defined from the reference Velocity Patterns, both for each individual velocity and for the Center of Gravity of the profile.

The meter then :

- selects the reference pattern at closest flowrate and Profile Number,
- checks if the current pattern match the reference within the defined limits,
- decides for the indicator accordingly.

The information is available as a contact at meter terminals for use by supervision system (logging and alarm).

Figure 12 - the CPM indicator

BLUE	Excellent profile match. Meter probably within +/- 0.10% from calibration.
GREEN	Meter within fiscal accuracy +/- 0.15% from calibration.
RED	Meter out of fiscal accuracy (does not mean out-of-service !)

7 OPEN QUESTIONS / FUTURE WORKS

- Currently running :

- Improve the knowledge of the acceptance limits.
- Extend the database of couples [Velocity Patterns / Meter Factors].

- Medium term :

- Speed up research on the tomographic approach.

7 CONCLUSIONS

- 1/ As off-site calibration of USMs is more and more considered, securing the transition from calibration laboratory to field is of primary concern.
- 2/ To achieve this, new control methods and procedures are required, as recommended by API MPMS.
- 3/ These methods can be successfully implemented on the meters of new generation, thanks to their large number of beams giving a rich and reliable access the velocity profile.